DESIGN OF A NEW HIGH-PERFORMANCE

POINTING CONTROLLER

FOR THE HUBBLE SPACE TELESCOPE

Final Report

3 August, 1992 through 3 October, 1993

Prepared by

Dr. C. D. Johnson
Electrical and Computer Engineering Dept.
University of Alabama in Huntsville
Huntsville, Alabama 35889

October 1993

NASA

National Aeronautics and Space Administration

Report Documentation Page

1. Report No. 1	2. Government Accession No.	3. Recipient's Catalog No.
4. Title and Subtitle Design of a New High-Performance Pointing Controller for the Hubble Space Telescope		5. Report Date October 1993
		6. Performing Organization Code
7. Author(s) Dr. C. D. Johnson		8. Performing Organization Report No.
		10. Work Unit No. D.O. # 49
9. Performing Organization Name and Address University of Alabama in Huntsville, ECE Dept. Huntsville, Alabama 35899		11. Contract or Grant No. NAS8-38609
		13. Type of Report and Period Covered FINAL: 8/3/92-10/3/93
12. Sponsoring Agency Name and Address National Aeronautics and Space Administration Washington, DC 20546-0001 Marshall Space Flight Center, Huntsville, AL 35812		14. Sponsoring Agency Code

16. Abstract

A new form of high-performance, disturbance-adaptive pointing controller for the Hubble Space Telescope (HST) is proposed. This new controller is all linear (constant gains) and can maintain accurate "pointing" of the HST telescope in the face of persistent, randomly triggered uncertain, unmeasurable "flapping" motions of the large attached solar array panels. Similar disturbances associated with antennas and other flexible appendages can also be accommodated. The effectiveness and practicality of the proposed new controller is demonstrated by a detailed design and simulation testing of one such controller for a planar-motion, fully nonlinear model of HST. The simulation results show a high degree of disturbance isolation and pointing stability.

17. Key Words (Suggested by Author(s)) Hubble Space Telescope Pointing Controller for HST Pointing Control System		18. Distribution Statement	
19. Security Classif. (of this report)	20. Security Classif. (of this page)	21. No. of pages	22. Price

NASA FORM 1626 OCT 86

DISCLAIMER

The views and opinions expressed in this report are those of the Principal Investigator and his collaborator, Mr. Stewart Addington, and are not necessarily the views and opinions of NASA, in general, or the Precision Pointing Systems Branch of Marshall Space Flight Center, in particular.

OVERVIEW OF THIS REPORT

This report describes a new methodology for designing a disturbance-adaptive, precision pointing controller for the Hubble Space Telescope (HST). The proposed new controller can maintain a consistent high-quality of pointing stability in the face of persistent, randomly triggered, "flapping" of the two large flexible solar arrays attached to either side of HST. Similar HST unknown, unmeasurable "disturbances" associated with deflections of other flex-body appendages (long, slender antenna booms, etc.) can also be accommodated by the same pointing controller.

A noteworthy feature of this new disturbance-adaptive pointing controller is that the structure of the controller algorithm is all linear, has all constant coefficients, and is relatively low-order, thus enhancing the controller's reliability and implementation attributes.

The effectiveness of the proposed new precision pointing control methodology is demonstrated in this report by a detailed design, and closed-loop simulation testing, of one such pointing controller for a planar-motion (single-axis), "exact" non-linear model of HST. The simulation results show a high-degree of pointing stability in the face of persistent flex-body "flapping" motions of the simulated solar arrays. A novel feature of the proposed controller is its dual-mode capability. In particular, the controller has the capability of switching into a special non-pointing control mode in which the pointing control actions "sway" the telescope's main-body in a series of back-and-forth motions that are automatically timed and orchestrated to induce "active damping" (damping augmentation) of the flapping solar arrays. This action results in a significant and rapid reduction of the solar array oscillations.

The rationale, general design procedure, and worked (single-axis) example for the proposed new dual-mode precision pointing controller is presented in Chapter 1 of this Report. Details of the derivation of the "exact," non-linear HST model (planar-motion) and the associated model equations are presented in the various Appendices of Chapter 1, along with various design formulae.

The scientific basis of the precision pointing controller design methodology proposed herein is relatively new and/or unfamiliar to some practicing control designers. Therefore, to aid such readers in becoming more familiar with the underlying scientific basis of our methodology, and to explain more fully why this new approach is essentially the "best" one can do in designing precision pointing/tracking controllers for systems operating in uncertain disturbance environments, a tutorial account of the control-theoretic principles of our methodology is presented in Chapter 2.

The detailed design and simulation results presented in this report were developed in collaboration with Mr. Stewart Addington, Graduate Student in the ECE Dept. of UAH; see also the Acknowledgment at the end of this chapter.

Chapter 1

DESIGN OF A NEW HIGH-PERFORMANCE
POINTING CONTROLLER
FOR THE HUBBLE SPACE TELESCOPE*

Chapter Summary

Cyclic thermal expansions and mechanical stiction effects in the Solar Arrays on the Hubble Space Telescope (HST) are triggering repeated occurrences of damped, relaxation-type flex-body vibrations of the solar arrays. Those solar array vibrations are, in turn, causing unwanted, oscillating disturbance torques on the HST main body, which cause unwanted deviations of the telescope from its specified pointing direction.

In this chapter we propose two strategies one can adopt in designing a telescope-pointing controller to cope with the aforementioned disturbances: (i) a "total isolation" (TI) control strategy whereby the HST controller torques are designed to adaptively counteract and cancel-out the persistent disturbing torques that are causing the unwanted telescope motions, and (ii) an "array damping" (AD) control strategy whereby the HST controller torques are used to actively augment the natural dampening of the solar array vibrations and the attendant telescope motions, between triggerings of the stiction-related flex-body relaxation oscillations.

Using the principles of Disturbance-Accommodating Control (DAC) Theory a dual-mode pointing controller for a generic, planar-motion

---

(single-axis) model of the HST is proposed. This pointing controller incorporates both the TI and AD modes of disturbance-accommodation. Simulation studies of the closed-loop system using generic parameter values clearly indicate, qualitatively, the enhanced pointing-performance such a controller can achieve.

1. *INTRODUCTION*

The two large deployable solar array panels attached, in a cantilever-beam fashion, to opposite sides of the Hubble Space Telescope (HST) main body (Figure 1) have introduced a new dimension to the problem of controlling the HST's pointing direction. In particular, the uneven thermal expansions of the solar array's collapsible structural members, caused by cyclic solar heating effects, and mechanical coulomb friction/stiction effects that resist thermal expansions between structural members are causing persistent, jerky, "flapping motions" of those solar arrays. Those flex-body flapping motions are of a damped-oscillation type and are triggered in a sporadic, random-like manner, depending on the intensity of the solar heating/cooling and on the varying stiction thresholds associated with sliding interactions between various structural members of the arrays.

These flapping motions of the solar arrays induce, through their attachment points with the main body of the HST, a series of randomly triggered damped-oscillation *disturbance torques* that cause the HST main body to veer away from the precision point needed to satisfy experiment requirements. Thus, an effective HST pointing control system must cope with this uncertain disturbance environment.

In this chapter we will derive a new conceptual form of HST pointing controller that effectively accomplishes this goal. Simulation results, using a non-linear, planar-motion model of the HST with generic parameter values,
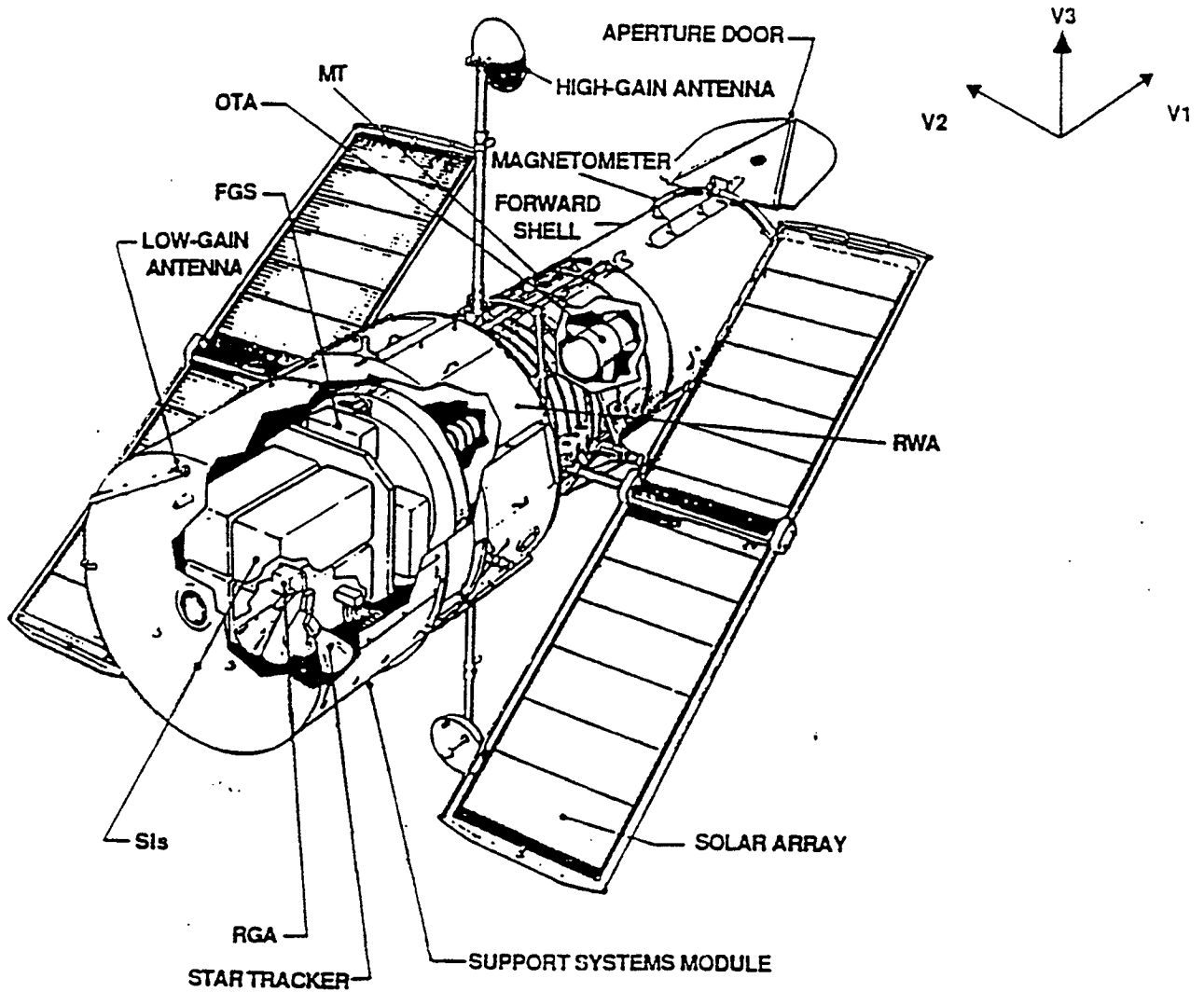
Fig. 1: The Hubble Space Telescope (HST) with Deployed Solar Arrays

demonstrate the effectiveness of the proposed new controller in a single-axis control context. A generalization of the control concepts presented here, to include full 3-axis pointing control of the HST, should provide a significant enhancement to the actual HST pointing performance.

2. CHARACTERIZATION OF THE SOLAR ARRAY FLAPPING DISTURBANCES IN THE HST CONTROL PROBLEM

The randomly-triggered flapping solar arrays pose a unique challenge to the HST control system design because the uncertain disturbance torques they induce to the HST main body are *not* effectively modeled as steady-state "random processes" with known *means* and *variances*. Consequently, traditional "stochastic control theories" [1] are ineffective in accomplishing high-performance, precision pointing of HST in the face of those flapping solar arrays.

The essential features of the HST uncertain disturbance torques due to flapping solar arrays are: (i) once triggered they have a distinguishable "damped-oscillation" type waveform characteristic that may have varying initial conditions, but is always relatively smooth and well-behaved (compared to the grossly jagged, erratic "white noise" of random process theory), and (ii) they are triggered in a once-in-a-while fashion with a relatively wide time-window between successive triggers (compared to the virtually continuous fusillade of triggering events associated with mathematical "white noise"). Thus, for instance, individual components (modes) $w_i(t)$ of the HST uncertain disturbance torques, due to the solar arrays, can be rather accurately represented (modeled) by a mathematical "spline" expression of the form

$$w_i(t) = C_1 e^{-\beta_i t} \sin(\omega_i t) + C_2 e^{-\beta_i t} \cos(\omega_i t) \qquad (1)$$

where $\beta_i>0$ denotes the damping parameter and $\omega_i>0$ denotes the oscillation frequency and where the spline "weighting-constants", C_1, C_2 in Eq.(1) are allowed to <u>jump in value</u> from time-to-time, in an uncertain, random-like manner (thereby allowing for different "initial conditions" on Eq.(1) at each triggering event). The numerical values of (β_i, ω_i) in Eq.(1) can be estimated from examination of actual flight data, results of ground experiments, etc.

It can be argued that, in practice, the parameters β_i, ω_i in Eq.(1) might be subject to some degree of uncertain, time-dependent variation due to wear, distortions, thermal effects, etc. which may render the model Eq.(1) ineffective. In such cases, an effective alternative to Eq.(1) is the considerably more robust polynomial-spline representation

$$w_i(t) = C_1 + C_2 t + C_3 t^2 + ... + C_m t^{(m-1)} \qquad (2)$$

where m is an appropriate positive integer and, as in Eq.(1), the "weighting-constants" $C_1, C_2,...,C_m$ are allowed to jump in value in an uncertain, once-in-a-while fashion, hereafter called "stepwise-constant" behavior. Expression Eq.(2) can effectively represent a broad class of uncertain, meandering-type disturbance functions $w_i(t)$, including complex "oscillations" of the type Eq.(1) with <u>completely unknown</u> waveform characteristics. In practice, satisfactory results using Eq.(2) can usually be achieved even with relatively small values for m, typically m = 3 or m = 4 (the so-called quadratic and cubic "spline models", respectively.)

In summary, individual modes of the uncertain disturbance torques associated with the flapping solar arrays on the HST have relatively smooth, well-behaved, time-domain waveform characteristics of the randomly triggered, damped-oscillation type. Consequently, those disturbance torques are effectively represented by mathematical "spline expressions" of the form

Eq.(1) or Eq.(2). It is remarked that in some situations, a *combination* of Eq.(1) and Eq.(2) may be most effective.

3. *ACCOMMODATION OF SOLAR ARRAY DISTURBANCES IN THE HST*

As stated earlier, the HST disturbance torques associated with flapping solar arrays cause the point of the HST main body to deviate from the desired direction. Thus, it is clear that those persistent disturbances cause only unwanted, upsetting effects. Consequently, the primary goal of the HST pointing controller, with respect to accommodating those disturbances, should be to (ideally) generate opposing control torques that automatically adapt-to and cancel-out (counteract) the persistent disturbance torques and their upsetting effects, in real-time. Under this latter mode of control, the main body of the HST would be effectively isolated from the disturbing motions of the flapping solar arrays, so that the point of the HST could then be regulated as if there were no solar array flapping motions. Hence, we hereafter refer to this control strategy as the total isolation (TI) mode of control.

In the TI mode of control, no effort is made to mitigate the flapping motions of the solar arrays themselves. However, the (mild) natural structural damping effects in the solar array structures will tend to dampen-out those oscillations--until such time that the oscillations are once again triggered by another thermal/stiction relaxation effect. In some situations, it may be desirable to employ the HST controller to hasten the natural damping-out of the solar array oscillations. This can be accomplished by designing the HST controller to create strategic rocking motions of the HST main body that are so timed and phased as to accomplish "active damping" (damping augmentation) of the solar array oscillations. We hereafter call this control strategy the array damping (AD) mode of control. Practical realization of the

AD mode of control would seem to require a relatively "smart" type of HST controller. However, it will be shown that a simple linear controller will do the job.

The TI and AD modes of control constitute what we believe to be the two main options to be considered in designing the HST pointing controller to accommodate uncertain disturbances such as oscillations of the solar arrays. For maximum flexibility in implementations, it is desirable to have a mode-switching arrangement for the TI/AD control laws, whereby one can gracefully shift control action from the TI mode to the AD mode (and vice-versa) in real-time, as dictated by the real-time needs on-station.

In the subsequent sections of this chapter we will demonstrate how a unique branch of modern control (Disturbance-Accommodation Control [DAC] Theory [2]-[6]) enables one to systematically design physically realizable, all linear, time-invariant controllers that embody the TI and AD modes of disturbance-accommodation described in this section.

4. *A SIMPLIFIED, PLANAR-MOTION CONFIGURATION MODEL OF THE HST*

The objective of this chapter is to develop, and demonstrate the performance characteristics of a new control concept for the HST pointing controller design. For this purpose, we will consider a simplified planar-motion (single-axis) generic configuration model of the HST, Figure 2, in which the inertias and flex-body (flapping) motions of the attached solar arrays are represented by rigid, movable arms attached to either side of the HST main body through idealized "pin-joints." To replicate one mode of the structural flexibility and structural damping effects of each of the solar arrays, the back-and-forth oscillations $\theta_1(t)$ $\theta_2(t)$ of the two arms about their respective pin-joints are considered to be resisted by linear torsional "spring"
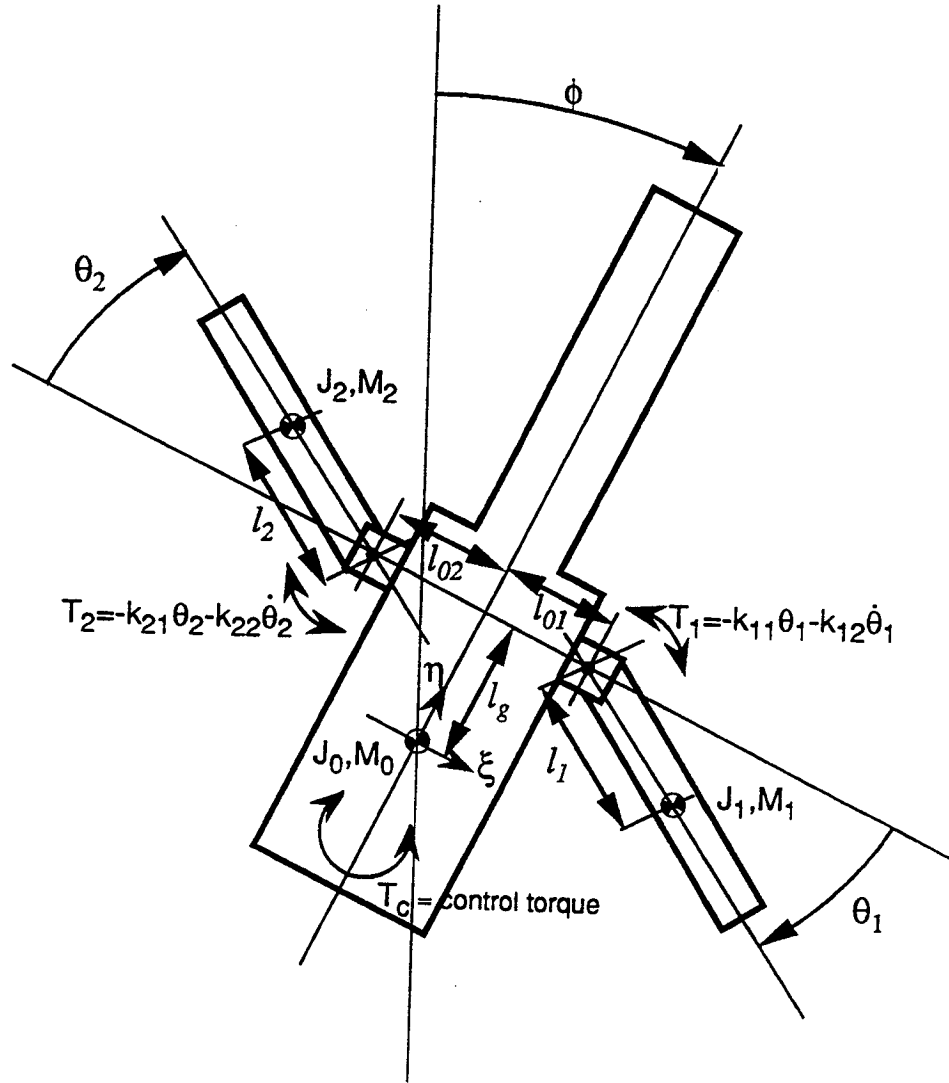
Fig. 2: Planar-Motion (Single-Axis) Configuration Model of HST and Attached Solar Arrays
(Replicating One Flex-Body Mode for Each Solar Array)

and linear viscous "damping" effects that may be *different* for each arm. The normal (equilibrium) positions of the arms are perpendicular to the HST main body.

To simultaneously replicate multiple flex-body modes of the solar arrays, one simply imagines multiple rigid arms attached to each of the two pin-joints in Figure 2, where the rotational spring constant damping mass and inertia of each arm is chosen to conform to the known frequency, damping and inertial properties of the particular flex-body mode being replicated. In this way one can consider as many simultaneous flex-body solar array modes (and flex-body modes of other HST appendages) as desired, using the pin-jointed rigid-arm technique as shown in Figure 3. Our decision to consider here only one flex-body mode, Figure 2, for each solar-array is motivated by the concept-demonstration nature of this chapter. In particular, we wish to avoid introducing additional complexity that is not essential to illustrating the basic concept of our modeling and control-design.

The planar-motion, concept-demonstration model in Figure 2 can be viewed as representing the actual HST when the solar arrays are rotated such that the flapping motions of each solar array consist of essentially one flex-body mode (which may be different for each array) and such that the associated disturbance torques induced to the HST main body cause relatively little out-of-plane rotational motions of the main body. The new controller scheme we develop here for the single-axis model in Figure 2 can be employed in each of the other two (rotational) axes (with proper coordination imposed between each such controller) to achieve full three-axis coordinated control of the HST main-body rotations for *arbitrary* positioning of the solar array panels.
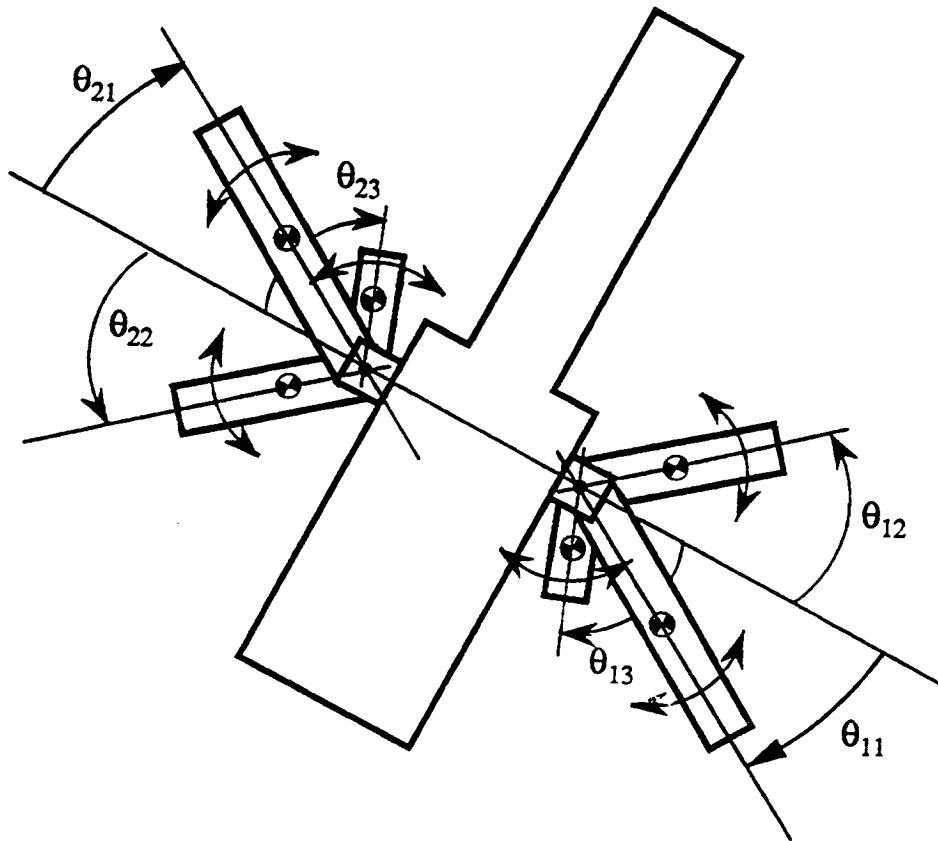
Fig. 3: Planar-Motion (Single -Axis) Configuration Model of HST and Attached Solar Arrays
(Replicating 3 Flex-Body Modes for Each Solar Array)

It is remarked that our introduction of the simplified, planar-motion HST configuration model in Figure 2 was not motivated primarily by a desire to keep things simple but, rather, by the technological necessity of having a mathematical model of HST that is based on "first principles" of dynamics. In particular, the ability to derive a controller that accomplishes the TI mode of disturbance-accommodation, as described in the previous section, requires that one begin with an HST mathematical model that embodies the actual dynamical equations of motion for the HST main body <u>and</u> for the "interface dynamics" associated with each of the attached solar arrays. Alternative mathematical models based on modal decompositions and/or transfer-function methodologies may not provide such detailed information and may "obscure" some novel control possibilities such as the TI mode of control we develop here.

5. *EXACT EQUATIONS OF MOTION FOR THE PLANAR-MOTION HST MODEL IN FIGURE 2*

The simplified, planar-motion HST configuration model in Figure 2 is, in fact, rather "complicated" from the dynamics point of view. In fact, the derivation of the exact equations of motion for Figure 2 would be extremely difficult and time-consuming using any of the classical methods of dynamics, such as Newton's, Lagrange's, or Hamilton's methods. For this study, the exact equations of motion for Figure 2 were derived, in completely general, explicit symbolic form, using the method of Kane's Equations [7] as implemented in the computer-aided modeling program Autolev©. The resulting mathematical model consists of a set of five (5) simultaneous, second-order, highly nonlinear, differential equations which can be written in the vector-matrix form

$$M(y)\ddot{y} + D\dot{y} + Ky + f(y,\dot{y}) = bu \qquad (3)$$

where y is the 5-vector of position variables $y = (\phi, \theta_1, \theta_2, \xi, \eta)$ as defined in Figure 2 and u is the (single-axis) HST main body control torque relevant to the planar-motion configuration shown in Figure 2. The elements of the 5x5 matrices {M(y), D, K} and of the vectors {b,f(y,ẏ)} in Eq.(3) are determined by various masses, inertias, lengths, etc., and their explicit expressions are given in Appendix A of this chapter. Those expressions are completely general in the sense that they are given in terms of arbitrary, symbolic masses, inertias, lengths, etc.

The natural dynamic behavior of the mathematical model Eq.(3) turns out to be surprisingly complicated, rich in diversity, and often counter-intuitive, owing to the strong, non-linear "inertia-coupling" that exists between the motions $\{\phi(t), \theta_1(t), \theta_2(t), \xi(t), \eta(t)\}$. That inertia coupling effect is manifested in the highly <u>non-sparse</u> structure of the non-constant, position-dependent "mass-matrix" M(y) in Eq.(3) which has the form (it turns out that $m_{ij} = m_{ij}(\theta_1, \theta_2)$, in general; see Appendix A of this chapter for explicit m_{ij} expressions)

$$
M = \begin{bmatrix}
m_{11} & m_{12} & m_{13} & m_{14} & m_{15} \\
m_{21} & m_{22} & 0 & m_{24} & m_{25} \\
m_{31} & 0 & m_{33} & m_{34} & m_{35} \\
m_{41} & m_{42} & m_{43} & m_{44} & 0 \\
m_{51} & m_{52} & m_{53} & 0 & m_{55}
\end{bmatrix}
\tag{4}
$$

We will now proceed to show how one can develop TI and AD pointing controllers for the HST model in Figure 2, based on the "exact" equations of motion Eqs. (3), (4).

accommodated by well-known, simple modifications of the results presented here.

Design of the TI mode of control begins by identifying the particular 2nd order equation of motion that governs the HST main-body rotation $\phi(t)$ in Figure 2. That equation can be obtained by first multiplying Eq.(3) by $M^{-1}(y)$ to obtain (the existence of M^{-1} is established in Appendix B of this chapter)

$$\ddot{y} + M^{-1}(y)D\dot{y} + M^{-1}(y)Ky + M^{-1}(y) f(y,\dot{y}) = M^{-1}(y)bu \qquad (5)$$

and then reading off the first of the five equations represented by Eq.(5). The result is the 2nd order, non-linear equation of motion

$$\ddot{\phi} + g(\theta_1, \theta_2, \dot{\theta}_1, \dot{\theta}_2, \dot{\phi}, \dot{\xi}, \dot{\eta}) = h(q_1, q_2)u \qquad (6)$$

where the precise expressions for the functions $g(\cdot)$, $h(\cdot)$ are given in Eqs. (C.2) and (C.3) of Appendix C of this chapter. Eq.(6) governs the actual angular motions $\phi(t)$ of the HST main body as shown in Figure 2, for an arbitrary control torque input $u(t)$. Note that the one term $g(\cdot, \cdot, \cdot)$ in Eq.(6) embodies all of the disturbing torques induced on the HST main body by the flapping motions of the solar arrays in Figure 2.

At this point, it is useful to introduce the notion of an ideal-model for the desired controlled (closed-loop) motions of the pointing angle $\phi(t)$, in the TI mode of control. For this purpose, we assume the desired transient behavior of $\phi(t)$ in the TI mode is represented by the solutions of the specified (given) "ideal-model differential equation"

(Ideal Model Eq.) $\qquad \ddot{\phi} + (2\zeta\omega_n)\dot{\phi} + (\omega_n^2)\phi = 0 \qquad (7)$

where the values of the parameters ($\zeta > 0$, $\omega_n > 0$) are assumed specified. Thus, the control designer's task is to design the control function $u=u(?)$ in Eq.(6) to make Eq.(6) "look like" Eq.(7). In the idealistic case, where all

arguments in $g(\cdot)$, $h(\cdot)$ can be accurately measured in real-time, it is clear that the ideal choice for the TI controller $u(\cdot)$ in Eq.(6) would be

$$u = h^{-1}(\theta_1, \theta_2) [-k_2 \dot{\phi} - k_1 \phi + g(\theta_1, \theta_2, \dot{\theta}_1, \dot{\theta}_2, \phi, \dot{\xi}, \dot{\eta})] \qquad (8,a)$$

where

$$k_1 = \omega_n^2 \quad ; \quad k_2 = 2\zeta \omega_n. \qquad (8,b)$$

However, for this study it is assumed that only $\phi(t)$ can be measured in real-time. Thus we will seek a physically realizable approximation to Eq.(8) as follows. First, the term $h(\theta_1, \theta_2)$ in Eq.(6) will be approximated by a fixed constant $\hat{h}$ that is selected to approximate the range of values of $h(\theta_1, \theta_2)$ for a representative range of (θ_1, θ_2) values. (The determination of $\hat{h}$ is presented in Appendix B of this chapter.) Next, the function $g(\cdot,\cdot,\cdot)$ in Eq.(8) will be viewed and treated as an unknown, time-varying "disturbance" term $g(t)$ defined by

$$g(t) = g(\theta_1(t), \theta_2(t), \dot{\theta}_1(t), \dot{\theta}_2(t), \dot{\phi}(t), \dot{\xi}(t), \dot{\eta}(t)) \qquad (9)$$

where $\{\theta_1(t), \theta_2(t), \phi(t), \xi(t), \eta(t)\}$ are arbitrary solutions of the exact equations of motion Eq.(3). A typical time-plot of Eq.(9) is shown in Figure 4, where it can be seen that the unknown "disturbance" $g(t)$ is a smooth, well-behaved function that slowly meanders back and forth in an oscillating manner. We will now show how one can estimate the time-function $g(t)$ in real-time, from real-time measurements of $\phi(t)$. Thus, following the principles of Disturbance-Accommodating Control Theory [3, p. 412], we first represent the uncertain time-behavior of $g(t)$ by a quadratic polynomial-spline (See Eq.(2).)
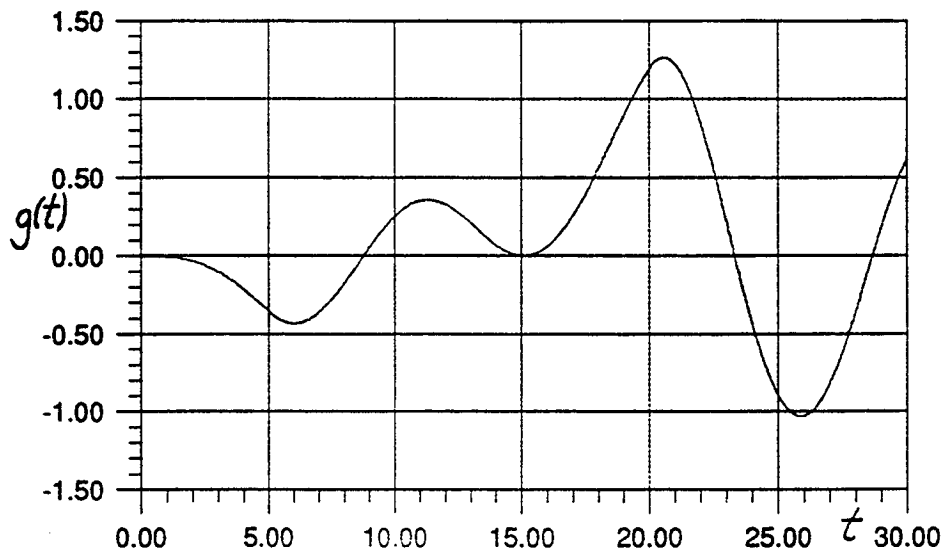
$$g(t) = C_1 + C_2 t + C_3 t^2 \qquad (10)$$

Fig 4: Typical Time-Plot of g(t) in Eq. (9).

where the weighting "constants" C_i in Eq.(10) are allowed to jump in a once-in-a-while, stepwise-constant manner, as described below Eq.(2). Next we introduce a *state-variable model* for g(t) by defining

$$z_1 = g(t) \quad ; \quad z_2 = \dot{g}(t) \quad ; \quad z_3 = \ddot{g}(t) \quad (11)$$

and observing that the z_i obey the following differential equations

$$\dot{z}_1 = z_2 + \sigma_1(t) \quad ; \quad \dot{z}_2 = z_3 + \sigma_2(t) \quad ; \quad \dot{z}_3 = \sigma_3(t) \quad (12)$$

where the symbols $\sigma_i(t)$ in Eq.(12) denote totally <u>unknown, unmeasurable,</u> sparsely populated time-sequences of randomly-arriving, random-intensity impulses (Dirac impulses). Those impulses represent the "cause" of the once-in-a-while jumping of the C_i values in Eq.(10).

The foregoing arguments and approximations enable us to rewrite the exact equation of motion Eq.(6) for $\phi(t)$ in the approximate and simplified form

$$\ddot{\phi} = \hat{h}u - w(t) \quad ; \quad \hat{h} \approx h \quad ; \quad w(t) = g(t) \quad (13)$$

where, according to Eq.(11), the "disturbance" term $w(t)$ in Eq.(13) is given by

$$w(t) = z_1(t) \quad (14)$$

and where $z_1(t)$ is (approximately) governed by the set of impulse-forced differential equations Eq.(12). The TI control law (8) corresponding to (13) thus becomes the constant-gain linear control law

$$u = \hat{h}^{-1} [-k_2 \hat{\dot{\phi}} - k_1 \phi + \hat{z}_1(t)] \quad (15)$$

where k_1, k_2 are defined as in (8b) and where, following standard DAC techniques [3, p. 430], $\hat{\dot{\phi}}(t)$ and $\hat{z}_1(t)$ denote on-line, real-time estimates of $\dot{\phi}(t)$ and $z_1(t)$ obtained from a composite plant/disturbance state-observer (Kalman filter), based on the approximate plant-model Eq.(13), and the "disturbance" model, Eq.(12). That composite state-observer operates on the plant output measurement $\phi(t)$ and plant control input $u(t)$ to produce accurate

real-time estimates of the state-variables $\{x_1 = \phi, x_2 = \dot{\phi}\}$ for the <u>actual</u> plant Eq.(6), as well as estimates of the state-variables $\{ z_1 = g(t), z_2 = \dot{g}(t), z_3 = \ddot{g}(t) \}$ for the "disturbance" term $w(t)$ in Eq.(13). The design of the composite state-observer for this TI mode of control is described in Appendix C of this chapter.

Substituting the control expression Eqs. (15), (8b) into the <u>actual</u> equation of motion, Eq.(6), yields the actual, closed-loop equation of motion for $\phi(t)$ in the TI mode as

$$\ddot{\phi} + g(\cdot,\cdot,\cdot) = h(\cdot,\cdot)\hat{h}^{-1} [-k_2 \hat{\dot{\phi}} - k_1\phi + \hat{z}_1(t)] \tag{16}$$

which can be rearranged to read

$$\ddot{\phi} + h\,\hat{h}^{-1} [(2\zeta\omega_n)\hat{\dot{\phi}} + (\omega_n{}^2) \phi] = -g(\cdot,\cdot) + h\,\hat{h}^{-1}\,\hat{z}_1(t) \tag{17}$$

Comparison of Eq.(17) with Eq.(7) shows that the desired ideal-model behavior of $\phi(t)$ in the TI mode of control will be realized, provided the assumed approximations

$$h(\cdot,\cdot)\hat{h}^{-1} \approx 1 \quad ; \qquad \hat{\dot{\phi}} \approx \dot{\phi}(t) \tag{18a}$$

$$\hat{z}_1(t) \approx g(\theta_1(t),\theta_2(t),\dot{\theta}_1(t),\dot{\theta}_2(t),\dot{\phi}(t),\dot{\xi}(t),\dot{\eta}(t)) \tag{18b}$$

are achieved by the aforementioned design procedure. This completes the design of the HST controller for the TI mode of control.

Design of the AD Controller

The TI mode of control automatically isolates the HST main-body from any disturbance torques induced by the flapping solar arrays and is therefore proposed as the <u>normal</u> control mode for HST pointing experiments. On the other hand, one can imagine exceptional situations in which the prompt damping of excessive solar array oscillations becomes a primary concern. For those situations, the Array Damping (AD) mode of control provides a means for <u>actively</u> augmenting the natural damping of the solar array

oscillations by carefully controlled and orchestrated dynamic motions of the HST main body. To achieve this active augmentation to the solar arrays' natural structural damping effects, the AD controller must maneuver the HST main-body motions $\phi(t)$ back and forth, so as to induce controlled, time-varying, "bending torques" [at the body/solar array attachment point (structural interface)] that are strategically timed to dissipate the energy of the oscillating solar arrays themselves. It is rather surprising that this seemingly complex, intricate control task can be accomplished by a simple, constant-gain, linear controller, as we shall now show.

The design of the AD mode of control begins by identifying the particular sub-set of the complete equations of motion, Eq. (3), that governs the motions $\phi(t)$, $\theta_1(t)$, $\theta_2(t)$. That particular sub-set consists of the first three 2nd order differential equations in Eq.(5), which can be separated out from (3) and be written as

$$\ddot{\bar{y}} + \overline{D}(\bar{y})\dot{\bar{y}} + \overline{K}(\bar{y})\bar{y} + \bar{f}(y,\dot{y}) = \overline{b}(\bar{y})u \qquad (19)$$

where $\bar{y} = (\phi, \theta_1, \theta_2)$ and where $\overline{D}(\bar{y})$, $\overline{K}(\bar{y})$, $\bar{f}(y,\dot{y})$, $\overline{b}(\bar{y})$ can be determined from $M^{-1}D$, $M^{-1}K$, etc. in Eq. (5). Next, one must <u>linearize</u> Eq. (19) in the neighborhood of the anticipated "operating-point" values of $\{\phi(t), \theta_1(t), \theta_2(t)\}$. For our problem those operating point values are

$$\phi = \dot{\phi} = 0 \quad ; \quad \theta_1 = \dot{\theta}_1 = 0 \quad ; \quad \theta_2 = \dot{\theta}_2 = 0 \qquad (20)$$

Linearizing Eq. (19) in the neighborhood of Eq. (20), using standard procedures, then yields Eq. (19) in the <u>linear, constant-coefficient</u> form [Note: $\bar{f}(y,\dot{y}) = 0$ at $\phi = \dot{\phi} = \theta_1 = \dot{\theta}_1 = \theta_2 = \dot{\theta}_2 = 0$]

$$\ddot{\bar{y}} + \tilde{D}\dot{\bar{y}} + \tilde{K}\bar{y} = \tilde{b}u \qquad (21)$$

where $\{\ \tilde{D}, \tilde{K}, \tilde{b}\ \}$ denote the values of $\{\overline{D}(\overline{y}), \overline{K}(\overline{y}), \overline{b}(\overline{y})\}$ at the operating values Eq.(20). In the AD control mode the objective is to <u>simultaneously</u> achieve the three stabilization conditions

$$\phi(t) \rightarrow 0 \quad ; \quad \theta_1(t) \rightarrow 0 \quad ; \quad \theta_2(t) \rightarrow 0 \tag{22}$$

For this purpose we first seek $u(\cdot)$ in the (idealistic) constant-gain linear state feedback form

$$u = k_c^T \left(\frac{\overline{y}}{\dot{\overline{y}}} \right) = k_{c1}\phi + k_{c2}\theta_1 + k_{c3}\theta_2 + k_{c4}\dot{\phi} + k_{c5}\dot{\theta}_1 + k_{c6}\dot{\theta}_2 \tag{23}$$

where the six elements of the control gain-vector $k_c = (k_{c1}, \dots, k_{c6})$ are chosen to place the corresponding six (closed-loop) eigenvalues $\{\lambda_1, \dots, \lambda_6\}$ of Eq. (21) at suitably "stable" locations in the complex plane. An effective procedure for computing the gains $\{k_{c1}, \dots, k_{c6}\}$, for any given set of desired eigenvalues $\{\lambda_1, \dots, \lambda_6\}$, is outlined in Appendix C. For our simulation studies, we selected the six λ_i to consist of <u>three identical pairs</u> of stable, complex-conjugate roots defined by

$$\lambda_{1,2} = -\zeta\omega_n \pm j\omega_n\sqrt{1-\zeta^2} \quad ; \quad j = \sqrt{-1} \quad , \tag{24}$$

where $(\zeta > 0,\ \omega_n > 0)$ are chosen to yield satisfactory closed-loop response characteristics for the AD mode.

The final step in the design of the AD control mode is to develop a state-observer (Kalman filter) that generates accurate real-time estimates of $\phi(t)$, $\theta_1(t)$, $\dot{\theta}_1(t)$, $\theta_2(t)$, $\dot{\theta}_2(t)$ from the available measurement $\phi(t)$, as needed to implement the AD control law Eq. (23). For this purpose we developed a conventional full-order observer based on the linearized model Eq. (21). The details of that observer design are presented in Appendix C of this chapter. The outputs $\hat{\phi}, \hat{\theta}_1, \hat{\dot{\theta}}_1, \hat{\theta}_2, \hat{\dot{\theta}}_2$ of that observer are used in place of their

idealized counterparts in Eq. (23) for implementation of the AD control mode. This completes the design of the HST controller for the AD mode of control.

7. SUMMARY OF THE PROPOSED NEW DUAL-MODE DISTURBANCE-ACCOMMODATING POINTING CONTROLLER FOR THE HST

The new HST pointing controller proposed in this study, for the single-axis model in Figure 2, consists of two distinct controller-algorithm configurations, one for the *total isolation* (TI) mode of control and one for the *array damping* (AD) mode of control. The TI controller is given by Eq.(15) and its associated state-observer [Appendix C, Eq. (C.13)], where the parameters (ζ, ω_n) are assumed chosen to yield the desired quality of closed-loop regulation response $\phi(t) \to 0$. The AD controller is given by Eq.(23) and its associated state observer [Appendix C, Eq. (C.26)], where the design parameters (ζ, ω_n) can be chosen to yield the desired "settling-time" for the actively augmented damping of the solar array oscillations.

In both the TI and AD modes of control, the presumed real-time plant output-measurements, for the planar-motion configuration of Figure 2, consist of the HST main-body pointing angle $\phi(t)$ only. If it should turn out that one can also accurately measure the rate $\dot{\phi}(t)$ in real-time, that additional measurement can be incorporated into the composite plant-state/disturbance-state observers associated with Eqs.(15) and (23); see Appendix C of this chapter.

In any consideration of a dual-mode controller, the question of how to gracefully "switch" from one mode to another naturally arises. In principle, such mode switchings are usually accomplished by a slow "fading" from one mode to another, similar to the way one "fades" signals from right to left speakers in a stereo sound system. However, this fading procedure must be

done in such a way that one control mode does not tend to "fight" the other control mode during the fading/mixing process. In this project it was found that a "fade" to the zero control level, in one control mode, was necessary before attempting to fade-into the other control mode. Otherwise one ran the risk of "fighting" developing between control modes during fading, as alluded to above. A further investigation of this issue seems warranted.

8. GENERIC PARAMETER VALUES FOR SIMULATION EXERCISES OF THE CLOSED-LOOP PLANAR-MOTION HST MODEL (FIGURE 2)

The numerical parameter values provided for the mathematical models supplied by NASA for this project were not appropriate for the alternative "first-principles," planar-motion dynamic model Eq. (3) we derived for our controller design procedure. Consequently, for our closed-loop simulation studies of the HST model in Figure 2, we chose a set of numerical parameter values, (for the various masses, inertias, length, etc. indicated in the configruration model of Figure 2 and in the analytical model Eq.(3)) which seem to be representative of the relative scale of values associated with the real-life HST. As a matter of fact, since our "exact" model Eq.(3) is derived in symbolic mass, inertia etc. parameter terms, and our controller design procedure is likewise expressed in terms of those same symbolic terms, it is a simple matter to re-evaluate our controller expressions and our simulation results for any given numerical values of HST/Solar Array parameter terms. Accordingly, the following two sets of numerical parameter values for Figure 2 were chosen for our simulation studies.

For both the symmetric and asymmetric solar array cases

$$l_{01} = 2.5 \text{ m} \qquad ; \qquad l_{02} = 2.5 \text{ m} \qquad ; \qquad l_g = 1.5 \text{ m}$$

$$l_1 = 4.8 \text{ m} \qquad ; \qquad l_2 = 4.8 \text{ m}$$

$$M_0 = 10,5000 \text{ kg} \quad ; \qquad J_0 = 10,5000 \text{ kgm}^2$$

$$M_1 = 180 \text{ kg} \qquad ; \qquad J_1 = 180 \text{ kgm}^2$$

$$M_2 = 180 \text{ kg} \qquad ; \qquad J_2 = 180 \text{ kgm}^2 \qquad\qquad (25)$$

For the case of dynamically <u>symmetric</u> solar arrays

<u>At the 0.6 Hz. flex-mode.</u>

$$k_{11} = 5.5 \qquad ; \qquad k_{12} = 0.001$$

$$k_{21} = 5.5 \qquad ; \qquad k_{22} = 0.001 \qquad\qquad (26a)$$

<u>At the 0.11 Hz. flex-mode.</u>

$$k_{11} = 0.18 \qquad ; \qquad k_{12} = 0.001$$

$$k_{21} = 0.18 \qquad ; \qquad k_{22} = 0.001 \qquad\qquad (26b)$$

For the case of dynamically <u>asymmetric</u> solar arrays

<u>At the 0.6 Hz. flex-mode.</u>

$$k_{11} = 6.5 \qquad ; \qquad k_{12} = 0.01$$

$$k_{21} = 5.5 \qquad ; \qquad k_{22} = 0.001 \qquad\qquad (26c)$$

<u>At the 0.11 Hz. flex-mode.</u>

$$k_{11} = 0.3 \qquad ; \qquad k_{12} = 0.001$$

$$k_{21} = 0.18 \qquad ; \qquad k_{22} = 0.001 \qquad\qquad (26d)$$

The set of HST *controller* parameter values chosen for use with Eqs.(25),(26) are:

For the TI control mode:

$$\zeta = 0.9 \qquad ; \qquad \omega_n = 1.0 \tag{27}$$

For the AD control mode

$$\zeta = 0.7 \qquad ; \qquad \omega_n = 1.0 \tag{28}$$

9. RESULTS FROM CLOSED-LOOP SIMULATION EXERCISES OF THE HST MODEL, EQ. (3)

The "exact" non-linear model Eq.(3) associated with Figure 2 was simulated and exercised in a series of runs on a digital computer, using the two cases of plant parameter values shown in Eqs.(25),(26). In that series of simulation exercises, the control term u in Eq. (3) was implemented, first as the TI controller Eq. (15) and associated state-observer, and then as the AD controller Eq. (23) and its associated state-observer, using the corresponding controller parameter values shown in Eqs.(27), (28). To demonstrate the ultimate performance capabilities of the TI and AD control modes, control actuator saturation effects were not simulated in these concept-demonstration exercises. The simulated excitation of the solar array oscillations was accomplished by applying random, once-in-a-while, short-duration, high-intensity external torque pulses (simulated torque "impulses") to one or the other of the solar-array arms shown in Figure 2. The resulting angular motions $\phi(t)$, $\theta_1(t)$, $\theta_2(t)$ of the HST main-body and flapping solar arrays, for both the TI control mode and the AD control mode, and for both the symmetric and the asymmetric solar array cases, are shown in the series of time-plots presented in Figs. 5-7. The time-plots in Figure 5 clearly show the TI controllers' ability to quickly adapt to, and counteract, the time-varying

disturbance torques induced by the vibrating solar arrays and thereby

THIS SPACE IS INTENTIONALLY LEFT BLANK

Fig. 5a: Closed-Loop Response of ϕ(t).

Fig. 5b: Closed-Loop Response of θ₁(t).

Fig. 5c: Closed-Loop Response of θ₂(t).

Fig. 5: Closed-Loop Responses for the TI Control Mode with Dynamically Asymmetric SA's
[0.11 Hz. SA oscillation triggered at t = 3.0 secs.]

1-26

Fig. 6a: Closed-Loop Response of φ(t).

Fig. 6b: Closed-Loop Response of θ₁(t).
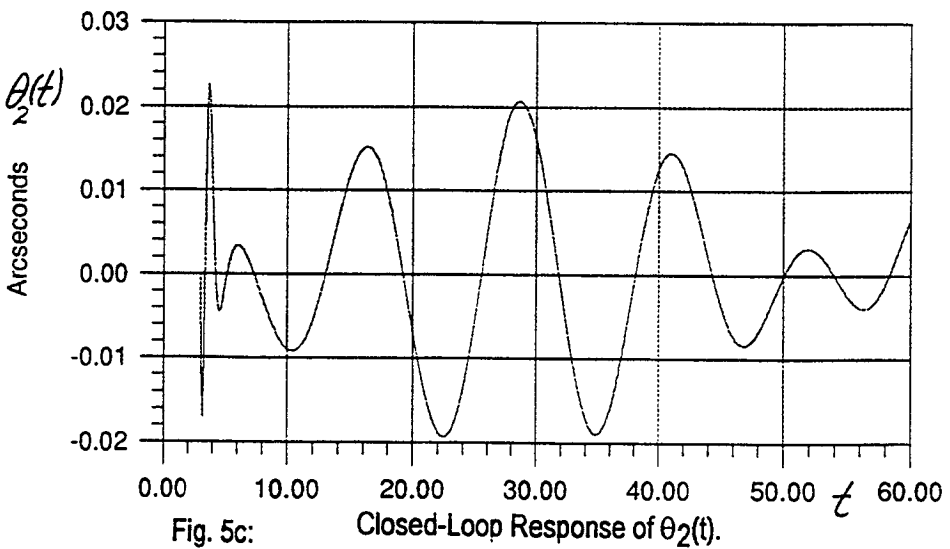
Fig. 6c: Closed-Loop Response of θ₂(t).

Fig. 6: Closed-Loop Responses for the AD Control Mode with Dynamically Asymmetric SA's
[0.6 Hz. SA oscillation triggered at t = 3.0 secs.]

1-27

Fig 7a: Closed-Loop Response of φ(t).

Fig.7b: Closed-Loop Response of θ₁(t).

Fig. 7c: Closed-Loop Response of θ₂(t).
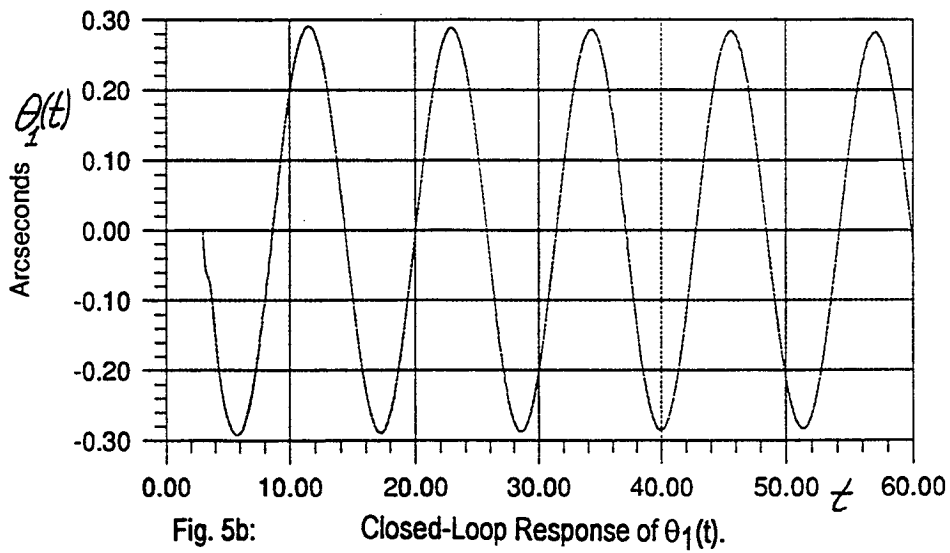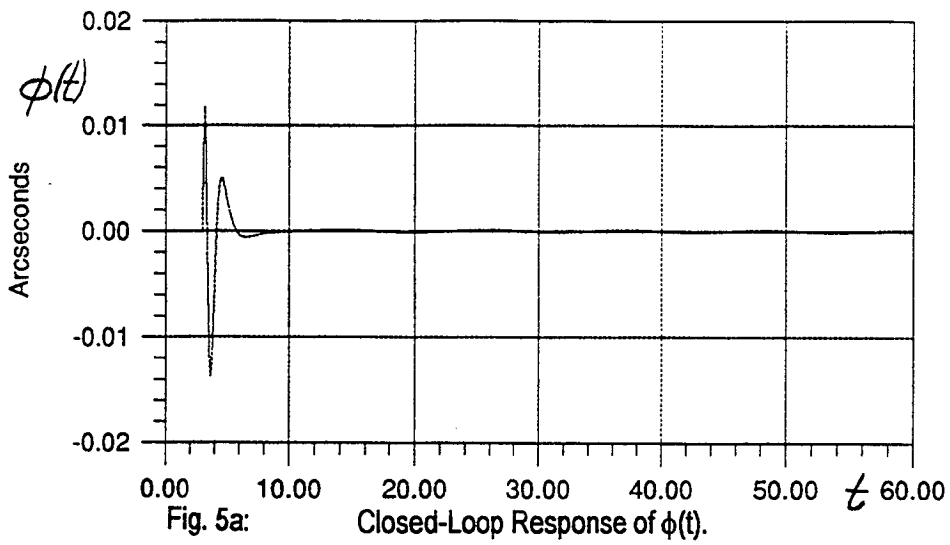
Fig.7:   Closed-Loop Responses for the Ad Control Mode with Dynamically Symmetric SA's
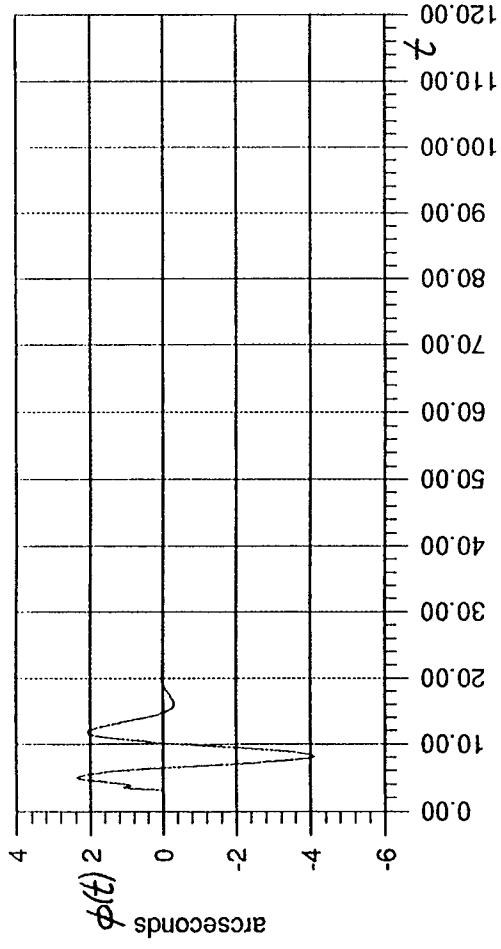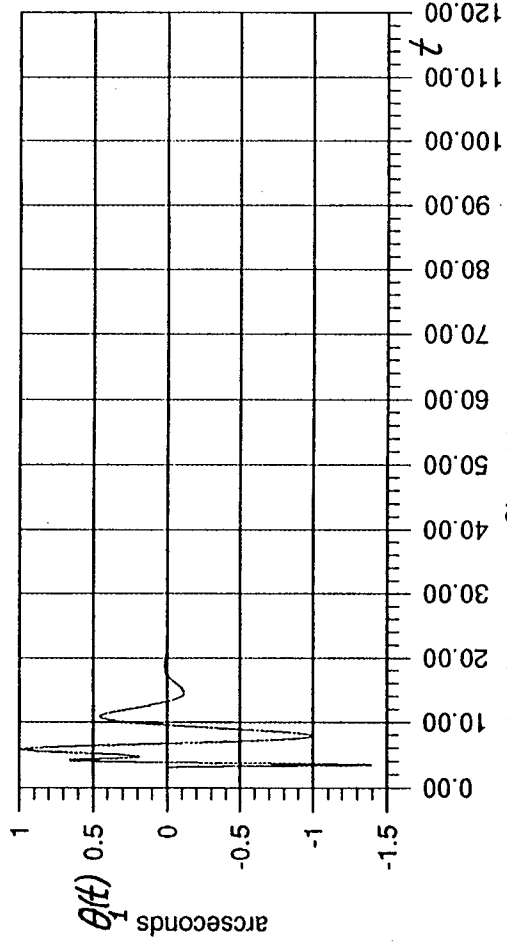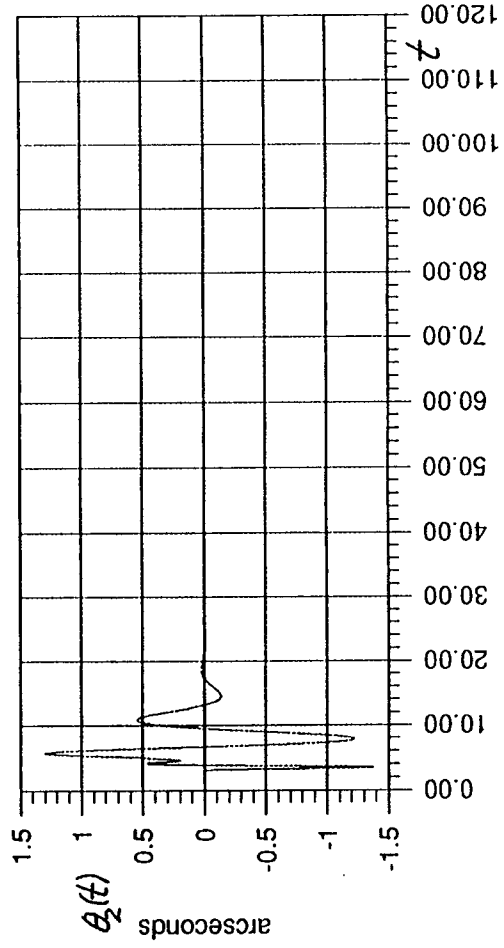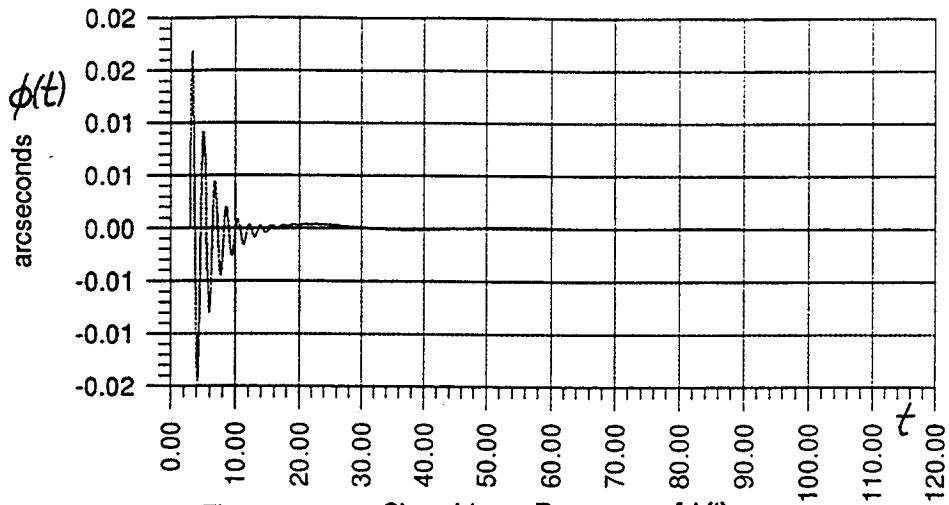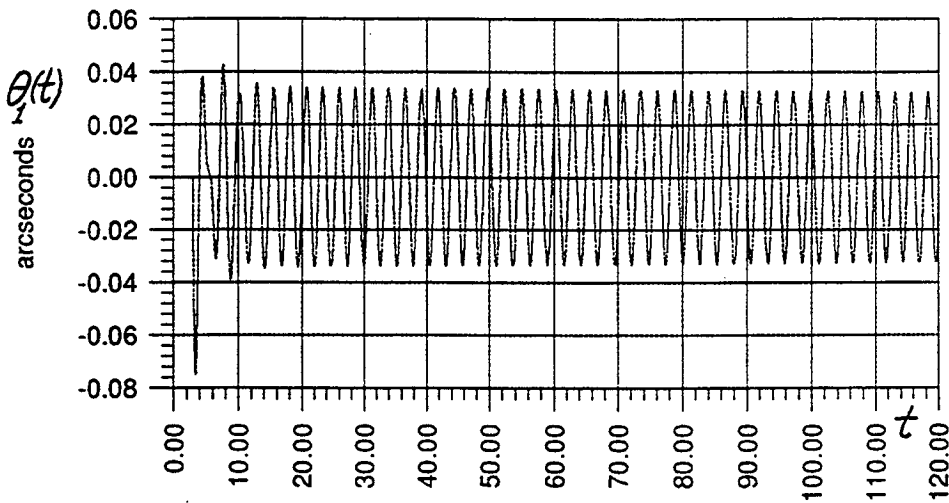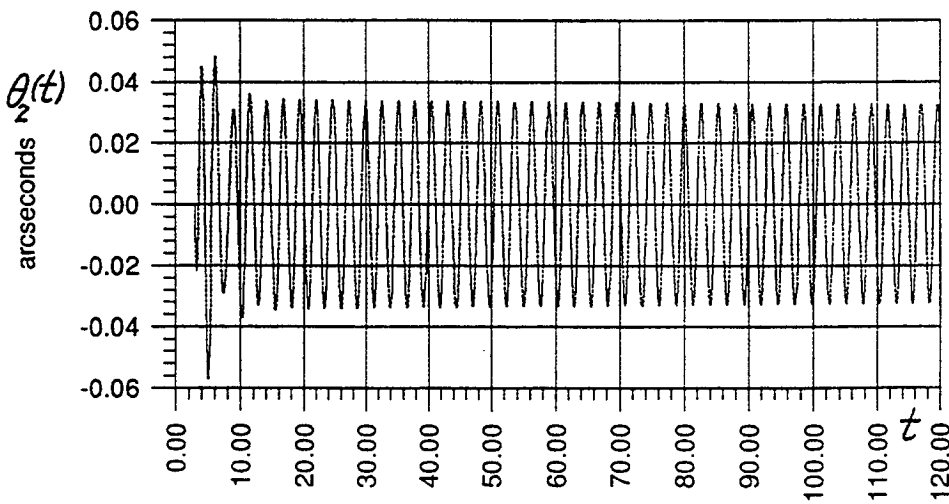[0.6 Hz. SA oscillation triggered at t = 3.0 secs.]

effectively isolate the HST main-body from those disturbances, while maintaining a high-quality of pointing set-point regulation $\phi(t) \approx 0$.

The closed-loop performances of $\phi(t)$, $\theta_1(t)$, $\theta_2(t)$, corresponding to the AD control mode are shown in Figs. 6-7. Those time-plots demonstrate the ability of the AD controller to strategically maneuver the HST main-body motion $\phi(t)$ so as to actively augment the natural structural damping in the solar arrays and thereby hasten the rate at which $\theta_1(t) \to 0$, $\theta_2(t) \to 0$. It is interesting to note that in the case of perfectly <u>symmetric</u> solar arrays, Figure 7, the AD controller cannot distinguish which of the two solar arrays is causing the disturbing torques (i.e. a disturbance <u>un</u>observability condition arises in the composite plant/disturbance state-observer used in the AD controller; see Appendix D of this chapter) and thus the AD controller cannot decide to which solar array it should direct the damping augmentation effort. Nevertheless, in that singular case, the AD controller automatically proceeds to maneuver the HST main-body so that the two solar arrays are coerced into flapping in an equal-but-opposite (birdwing-like) manner, $\theta_1(t) \equiv - \theta_2(t)$, so that the corresponding <u>net</u> torque disturbance induced to the HST main body is thereby damped to zero, while $\theta_1(t) \to 0$ and $\theta_2(t) \to 0$ according to their <u>natural</u> damping characteristics.

When the two solar arrays are simulated as *asymmetric*, the AD controller succeeds in individually augmenting the natural damping of both $\theta_1(t) \to 0$ and $\theta_2(t) \to 0$ as evidenced in Figure 6. It is remarked that the AD mode of control, as presently developed, exhibits a relatively small domain of (closed-loop) stability and tends to be rather sensitive to system parameter variations. These undesirable features, which appear to be a consequence of the non-linear behavior of the terms $M^{-1}(y)b$ and $M^{-1}(y) f(y,\dot{y})$ in the basic

plant model Eq.(5), rather than a characteristic of the AD controller itself, constitute an important area for further research.

10. *A COMPUTER-ANIMATION VISUALIZATION OF THE SIMULATED HST CLOSED-LOOP RESPONSE DYNAMICS*

The unique performance characteristics associated with the TI and AD control modes are dramatically evidenced by viewing a computer-generated animation of the controlled movements of the 3-body HST model (main-body and two attached "arms" representing the two solar arrays) as depicted in Figure 2. For this purpose, the normal simulation data { $\phi(t)$, $\theta_1(t)$, $\theta_2(t)$ } was input into a specially prepared computer graphics program which repeatedly "draws" frames of Figure 2 for a sequence of closely spaced discrete-time values t_k, $k = 0,1,2,3, ...$. When that set of frames is displayed on the computer monitor in rapid sequence, one can "see" the three interconnected component bodies in Figure 2, "moving" in planar-motion just as they would in reality. The intricate maneuvers of $\phi(t)$ one can thereby "see" being performed by the HST main-body, in the TI and AD control modes, are rather impressive.

11. *SUMMARY, CONCLUSIONS, AND RECOMMENDATIONS FOR FURTHER WORK*

In this chapter we have developed, and demonstrated by simulation exercises, a new dual-mode HST control concept for accommodating time-varying, persistent, uncertain torque disturbances (such as those due to flex-body "flapping" of the solar arrays) that act on the HST main-body and degrade precision pointing of the HST. The new controller consists of two distinct control modes. In the Total Isolation (TI) control mode (envisioned as the primary mode of control), the HST control torques automatically synchronize with, and adapt to, the time-varying disturbance torques (in an

equal-but-opposite sense) to effectively counteract and cancel the effects of those disturbance torques in real-time. As a result, the HST main-body is dynamically "isolated" from the disturbance torques, thereby permitting high-quality, precision pointing of the HST in the face of such disturbances. The system closed-loop performance using the TI control mode exhibits a high-degree of robustness.

In the Array Damping (AD) control mode (likely to be used only occasionally, when not in a pointing experiment) the HST's control torques are used to strategically maneuver the angular rotations of the HST main-body in a rocking, back-and-forth manner so as to induce an active damping (damping augmentation) effect to the natural damping of the solar array flex-body oscillations and thereby hasten the damping-out of those flex-body oscillations. When the AD control mode is used, the closed-loop system has the undesired feature of a relatively small domain of stability and relatively high sensitivities to system parameter variations, apparently due to the non-linear terms in the plant model, Eq. (5). A redesign of the AD controller to accommodate those non-linear terms should mitigate this feature.

The qualitative performance capabilities of the proposed new HST dual-mode controller concept have been determined by closed-loop computer simulation exercises. Those simulations are based on the exact, non-linear equations of motion for a simplified, planar-motion, 3-body configuration-model (Figure 2) of the HST and its solar arrays using a generic set of mass, inertia, and other parameter values that are considered to be scalewise representative of the actual HST and its solar array disturbances. As indicated earlier in this chapter, the HST numerical parameter-values made available to us for this study (by NASA, Marshall) were not relevant to the "exact", single-axis nonlinear model (3) we derived and used here. The

closed-loop performance capabilities exhibited in our simulation studies of the simplified (single-axis) HST model are considered to be representative of the performance that can be achieved for the actual HST, using a full 3-axis (angular axes) controller designed by the same methodology employed here. The recommendations for further work, listed below, are directed at efforts that will validate this claim.

Our recommendations for further work on the new HST pointing controller concept developed here are as follows:

1. Generalize the configuration-model (Figure 2) and the associated exact equations of motion, to include arbitrary, 3-axis, coupled angular motions for both the HST main body and the attached solar arrays. Include multiple modes of solar array oscillations.

2. Derive the 3-axis TI and AD controller equations corresponding to the generalized 3-axis model of HST. Generalize the AD controller equations to accommodate the non-linear terms in the HST model.

3. Revise the 3-axis TI and AD controller equations, as needed, for implementation in digital control format, [4].

4. Demonstrate the closed-loop performance of the 3-axis HST model, and associated 3-axis TI/AD controllers, by computer simulation exercises, using actual HST controller actuator saturation levels and realistic values for masses, inertia, and other HST / solar array model parameters.

5. Determine the most effective procedure for gracefully "fading" or "switching" from the TI control mode to the AD control mode, and vice versa.

ACKNOWLEDGMENT

The Principal Investigator and Mr. Addington would like to acknowledge the invaluable help of Mr. Mitchell Hunt, Ph.D. graduate student, UAH ECE Dept., who developed the HST computer animation program described herein.

REFERENCES

1. R. F. Stengel, *Stochastic Optimal Control; Theory and Applications*, John Wiley & Sons, New York, 1986.

2. C.D. Johnson, "Accommodation of Disturbances in Linear Regulator and Servomechanism Problems," *IEEE Trans. Auto. Cont.*, (Special Issue on Linear-Quadratic-Gaussian Problem), AC-16, No. 6, 1971, p.635.

3. C.D. Johnson, "Theory of Disturbance-Accommodating Controllers,: Chap. in *Control and Dynamic Systems: Advances In Theory and Applications, Vol. 23*, edited by C. T. Leondes, Academic Press, Inc., New York, 1976.

4. C.D. Johnson, "A Discrete-Time, Disturbance-Accommodating Control Theory for Digital Control of Dynamical Systems," Chap. in *Control and Dynamic Systems: Advances in Theory and Applications, Vol. 28*, Academic Press, New York, 1982.

5. C.D. Johnson, "Disturbance-Accommodating Control; An Overview, *Proc. 1986 Amer. Control Conf.*, Seattle, Wash., June 1986, pp. 526-536.

6. C.D. Johnson, "Effective Techniques for the Identification and Accommodation of Disturbances," *Proc. of 3rd NASA/DoD Controls-Structures Interaction Conference*, NASA Conf. Pub. No. 3041, p. 163, San Diego, CA, Jan. 19-Feb. 2, 1989.

7. T.R. Kane and David Levinson, *Dynamics; Theory and Applications*, McGraw-Hill, 1985.

APPENDICES

for

CHAPTER 1

APPENDIX A **THE EXACT EQUATIONS OF MOTION FOR THE PLANAR-MOTION MODEL OF FIG. 2**

The exact equations of motion for the planar-motion model of Fig. 2 were created by the AUTOLEV program and output as a FORTRAN simulation. The pertinent definitions in the source code were then copied to MATHEMATICA and reduced to generate the equations shown below. Computer simulations of these equations were performed with the original AUTOLEV generated code to preclude the introduction of copying errors.

For $\phi(t)$

$$
\begin{aligned}
-[J_0 &+ J_1 + J_2 + (l_{01}^2 + l_1{}^2 + l_g{}^2 + 2l_1(l_{01}\cos\theta_1 + l_g\sin\theta_1))M_1 \\
&+ (l_{02}^2 + l_2{}^2 + l_g{}^2 + 2l_2(l_{02}\cos\theta_2 - l_g\sin\theta_2))M_2]\ddot{\phi} \\
&- [J_1 + (l_1^2 + l_{01}l_1\cos\theta_1 + l_1 l_g\sin\theta_1)M_1]\ddot{\theta}_1 - [J_2 + (l_2^2 + l_{02}l_2\cos\theta_2 + l_2 l_g\sin-\theta_2)M_2]\ddot{\theta}_2 \\
&+ [(l_g + l_1\sin\theta_1)M_1 + (l_g - l_2\sin\theta_2)M_2]\ddot{\xi} + [-(l_{01} + l_1\cos\theta_1)M_1 + (l_{02} + l_2\cos\theta_2)M_2]\ddot{\eta} \quad (A.1) \\
= &-u + \dot{\phi}\dot{\xi}l_{01}M_1 + \dot{\eta}\dot{\phi}l_g M_1 - \dot{\phi}\dot{\xi}l_{02}M_2 + \dot{\eta}\dot{\phi}l_g M_2 \\
&+ (\dot{\phi}\dot{\xi} + 2\dot{\phi}\dot{\theta}_1 l_g + \dot{\theta}_1^2 l_g)l_1 M_1\cos\theta_1 + (\dot{\eta}\dot{\phi} - 2\dot{\phi}\dot{\theta}_1 l_{01} - \dot{\theta}_1^2 l_{01})l_1 M_1\sin\theta_1 \\
&- (\dot{\phi}\dot{\xi} + 2\dot{\phi}\dot{\theta}_2 l_g + \dot{\theta}_2^2 l_g)l_2 M_2\cos\theta_2 - (\dot{\eta}\dot{\phi} + 2\dot{\phi}\dot{\theta}_2 l_{02} + \dot{\theta}_2^2 l_{02})l_2 M_2\sin\theta_2
\end{aligned}
$$

For $\theta_1(t)$

$$
\begin{aligned}
-[J_1 &+ l_1^2 M_1 + l_{01}l_1 M_1\cos\theta_1 + l_1 l_g M_1\sin\theta_1]\ddot{\phi} - [J_1 + l_1^2 M_1]\ddot{\theta}_1 + [0]\ddot{\theta}_2 \\
&+ [l_1 M_1\sin\theta_1]\ddot{\xi} - [l_1 M_1\cos\theta_1]\ddot{\eta} \quad\quad (A.2) \\
= &-[J_1 + l_1^2 M_1][k_{11}\theta_1 + k_{21}\dot{\theta}_1] + l_1 M_1[(\dot{\phi}\dot{\xi} - \dot{\phi}^2 l_g)\cos\theta_1 + (\dot{\phi}\dot{\eta} + \dot{\phi}^2 l_{01})\sin\theta_1]
\end{aligned}
$$

For $\theta_2(t)$

$$
\begin{aligned}
-[J_2 &+ l_2^2 M_2 + l_{02}l_2 M_2\cos\theta_2 - l_2 l_g M_2\sin\theta_2]\ddot{\phi} + [0]\ddot{\theta}_1 - [J_2 + l_2^2 M_2]\ddot{\theta}_2 \\
&- [l_2 M_2\sin\theta_2]\ddot{\xi} + [l_2 M_2\cos\theta_2]\ddot{\eta} \quad\quad (A.3) \\
= &-[J_2 + l_2^2 M_2][k_{21}\theta_2 + k_{22}\dot{\theta}_2] + l_2 M_2[(-\dot{\phi}\dot{\xi} + \dot{\phi}^2 l_g)\cos\theta_2 + (-\dot{\phi}\dot{\eta} + \dot{\phi}^2 l_{02})\sin\theta_2]
\end{aligned}
$$

For $\xi(t)$ [translation of M_0 c.g. in ξ-direction]

$$
\begin{aligned}
[M_1(l_g &+ l_1\sin\theta_1) + M_2(l_g - l_2\sin\theta_2)]\ddot{\phi} + [l_1 M_1\sin\theta_1]\ddot{\theta}_1 - [l_2 M_2\sin\theta_2]\ddot{\theta}_2 - [M_0 + M_1 + M_2]\ddot{\xi} + [0]\ddot{\eta} \\
= &-[\dot{\eta}\dot{\phi}(M_0 + M_1 + M_2) + \dot{\phi}^2(l_{01}M_1 + l_{02}M_2) + \\
&\quad l_1 M_1(\dot{\phi}^2 + 2\dot{\phi}\dot{\theta}_1 + \dot{\theta}_1^2)\cos\theta_1 - l_1 M_1(\dot{\phi}^2 + 2\dot{\phi}\dot{\theta}_2 + \dot{\theta}_2^2)\cos\theta_2]
\end{aligned}
$$

$$(A.4)$$

For $\eta(t)$ [translation of M_0 c.g. in η-direction]

$$-M_1 l_1 [\cos\theta_1 - \cos\theta_2]\ddot{\phi} - [l_1 M_1 \cos\theta_1]\ddot{\theta}_1 + [l_1 M_1 \cos\theta_2]\ddot{\theta}_2 + [0]\ddot{\xi} - [M_0 + M_1 + M_2]\ddot{\eta}$$

$$= [\dot{\xi}\dot{\phi}(M_0 + M_1 + M_2) - \dot{\phi}^2 l_g (M_1 + M_2) - \quad\quad\quad\quad\quad\quad (A.5)$$

$$l_1 M_1(\dot{\phi}^2 + 2\dot{\phi}\dot{\theta}_1 + \dot{\theta}_1^2)\sin\theta_1 + l_2 M_2(\dot{\phi}^2 + 2\dot{\phi}\dot{\theta}_2 + \dot{\theta}_2^2)\sin\theta_2]$$

State Variables and the Equations of Motion. The equations of motion (A.1)-(A.5) can be represented by the standard second-order matric-vector equation for the planar-motion HST configuration in Fig. 2:

$$\mathbf{M}\ddot{y} + \mathbf{D}\dot{y} + \mathbf{K}y = \mathbf{b}u + f(y, \dot{y}) \quad\quad\quad\quad\quad\quad (A.6)$$

where

$$y = \begin{bmatrix} \phi, & \theta_1, & \theta_2, & \xi, & \eta \end{bmatrix}^\mathsf{T}$$

and the 25 elements $[\mathbf{M}]_{i,j}$ of $\mathbf{M}$ are given explicitly by

$$[\mathbf{M}]_{1,1} = -\big[J_0 + J_1 + J_2 + \{l_{01}^2 + l_1{}^2 + l_g{}^2 + 2l_1(l_{01}\cos\theta_1 + l_g\sin\theta_1)\}M_1$$

$$+ \{l_{02}^2 + l_2{}^2 + l_g{}^2 + 2l_2(l_{02}\cos\theta_2 - l_g\sin\theta_2)\}M_2\big]$$

$$[\mathbf{M}]_{1,2} = -\big[J_1 + (l_1^2 + l_{01}l_1\cos\theta_1 + l_1 l_g\sin\theta_1)M_1\big]$$

$$[\mathbf{M}]_{1,3} = -\big[J_2 + (l_2^2 + l_{02}l_2\cos\theta_2 - l_2 l_g\sin\theta_2)M_2\big]$$

$$[\mathbf{M}]_{1,4} = \big[(l_g + l_1\sin\theta_1)M_1 + (l_g - l_2\sin\theta_2)M_2\big]$$

$$[\mathbf{M}]_{1,5} = \big[-(l_{01} + l_1\cos\theta_1)M_1 + (l_{02} + l_2\cos\theta_2)M_2\big]$$

$$[\mathbf{M}]_{2,1} = -\big(J_1 + l_1^2 M_1 + l_{01}l_1 M_1\cos\theta_1 + l_1 l_g M_1\sin\theta_1\big)$$

$$[\mathbf{M}]_{2,2} = -\big(J_1 + l_1^2 M_1\big)$$

$$[\mathbf{M}]_{2,3} = 0$$

$$[\mathbf{M}]_{2,4} = l_1 M_1\sin\theta_1$$

$$[\mathbf{M}]_{2,5} = -l_1 M_1\cos\theta_1$$

$$[\mathbf{M}]_{3,1} = -\big(J_2 + l_2^2 M_2 + l_{02}l_2 M_2\cos\theta_2 - l_2 l_g M_2\sin\theta_2\big)$$

$$[\mathbf{M}]_{3,2} = 0$$

$$[\mathbf{M}]_{3,3} = -\big(J_2 + l_2^2 M_2\big)$$

$$[\mathbf{M}]_{3,4} = -\, l_2 M_2 \sin\theta_2$$

$$[\mathbf{M}]_{3,5} = l_2 M_2 \cos\theta_2$$

$$[\mathbf{M}]_{4,1} = \big[M_1 (l_g + l_1 \sin\theta_1) + M_2 (l_g - l_2 \sin\theta_2) \big]$$

$$[\mathbf{M}]_{4,2} = l_1 M_1 \sin\theta_1$$

$$[\mathbf{M}]_{4,3} = -\, l_2 M_2 \sin\theta_2$$

$$[\mathbf{M}]_{4,4} = -\,(M_0 + M_1 + M_2)$$

$$[\mathbf{M}]_{4,5} = 0$$

$$[\mathbf{M}]_{5,1} = -\, M_1 l_1 (\cos\theta_1 - \cos\theta_2)$$

$$[\mathbf{M}]_{5,2} = -\, l_1 M_1 \cos\theta_1$$

$$[\mathbf{M}]_{5,3} = l_1 M_1 \cos\theta_2$$

$$[\mathbf{M}]_{5,4} = 0$$

$$[\mathbf{M}]_{5,5} = -\,(M_0 + M_1 + M_2)$$

and where

$$\mathbf{D} = Diag\,\big[0, \quad (J_1 + l_1^2 M_1)k_{12}, \quad (J_2 + l_2^2 M_2)k_{22}, \quad 0, \quad 0 \big]$$

$$\mathbf{K} = Diag\,\big[0, \quad (J_1 + l_1^2 M_1)k_{11}, \quad (J_2 + l_2^2 M_2)k_{21}, \quad 0, \quad 0 \big]$$

$$\mathbf{b} = \big[1, \quad 0, \quad 0, \quad 0, \quad 0 \big]^{\mathsf{T}}$$

The elements f_i of the 5-vector $f(y, \dot{y})$ are given explicitly by

$$[f(y,\dot{y})]_1 = \dot{\phi}\dot{\xi}l_{01}M_1 + \dot{\eta}\dot{\phi}l_g M_1 - \dot{\phi}\dot{\xi}l_{02}M_2 + \dot{\eta}\dot{\phi}l_g M_2$$

$$+ (\dot{\phi}\dot{\xi} + 2\dot{\phi}\dot{\theta}_1 l_g + \dot{\theta}_1^2 l_g)l_1 M_1 \cos\theta_1 + (\dot{\eta}\dot{\phi} - 2\dot{\phi}\dot{\theta}_1 l_{01} - \dot{\theta}_1^2 l_{01})l_1 M_1 \sin\theta_1$$

$$- (\dot{\phi}\dot{\xi} + 2\dot{\phi}\dot{\theta}_2 l_g + \dot{\theta}_2^2 l_g)l_2 M_2 \cos\theta_2 - (\dot{\eta}\dot{\phi} + 2\dot{\phi}\dot{\theta}_2 l_{02} + \dot{\theta}_2^2 l_{02})l_2 M_2 \sin\theta_2$$

$$[f(y,\dot{y})]_2 = l_1 M_1 [(\dot{\phi}\dot{\xi} - \dot{\phi}^2 l_g)\cos\theta_1 + (\dot{\phi}\dot{\eta} + \dot{\phi}^2 l_{01})\sin\theta_1]$$

$$[f(y,\dot{y})]_3 = l_2 M_2 [(-\dot{\phi}\dot{\xi} + \dot{\phi}^2 l_g)\cos\theta_2 + (-\dot{\phi}\dot{\eta} + \dot{\phi}^2 l_{02})\sin\theta_2]$$

$$[f(y,\dot{y})]_4 = -\, \big[\dot{\eta}\dot{\phi}(M_0 + M_1 + M_2) + \dot{\phi}^2(l_{01}M_1 + l_{02}M_2) +$$

$$l_1 M_1 (\dot{\phi}^2 + 2\dot{\phi}\dot{\theta}_1 + \dot{\theta}_1^2)\cos\theta_1 - l_1 M_1 (\dot{\phi}^2 + 2\dot{\phi}\dot{\theta}_2 + \dot{\theta}_2^2)\cos\theta_2 \big]$$

$$[f(y, \dot{y})]_5 = [\dot{\xi}\dot{\phi}(M_0 + M_1 + M_2) - \dot{\phi}^2 l_g (M_1 + M_2) -$$

$$l_1 M_1 (\dot{\phi}^2 + 2\dot{\phi}\dot{\theta}_1 + \dot{\theta}_1^2) \sin\theta_1 + l_2 M_2 (\dot{\phi}^2 + 2\dot{\phi}\dot{\theta}_2 + \dot{\theta}_2^2) \sin\theta_2]$$

The term $Diag$ denotes a diagonal matrix with main diagonal shown. It should also be noted that the M matrix is strictly a function of θ_1 and θ_2 (the matrices D,K are constants for the model (A.1)-(A.5)). The ten state-variables for (A.6) can be chosen as $(x_1, \ldots, x_{10}) = (y, \dot{y})$.

Appendix B EXISTENCE OF M^{-1} AND DETERMINATION OF $\hat{h}$

The existence of the inverse of the mass matrix, M, and of the scalar $h = [\mathrm{M}^{-1}]_{1,1}$ over the range of θ_1, θ_2 values of interest, is easily established if the numerical values of the inertia, mass, and lengths in the planar-motion model are set. Using the parameter values (25) – (28) the determinant of M, for a representative range of θ_1, θ_2 values, varies as shown in Figures B-1. The variations in the h value for those same parameter values and the same range of θ_1, θ_2 values are as shown in Figure B-2. It is clear from Figures B-1 and B-2 that $det.\mathrm{M}$ and h are well-defined and strictly negative for the indicated range of θ_1, θ_2 values. The chosen approximating constant values for (M, h) are denoted by $(\hat{\mathrm{M}}, \hat{h})$.

For the linearization of (19) and design of the controller and observer gains, the representative constant values for $\hat{\mathrm{M}}$, $\hat{\mathrm{M}}^{-1}$ and $\hat{h}$ were determined to be:

$$\hat{\mathrm{M}} = \begin{bmatrix} -30854.4 & -6487.2 & -6487.2 & 540 & 0 \\ -6487.2 & -4327.2 & 0 & 0 & -864 \\ -6487.2 & 0 & -4327.2 & 0 & 864 \\ 540 & 0 & 0 & -10860 & 0 \\ 0 & -864 & 864 & 0 & -10860 \end{bmatrix} \tag{B.1}$$

$$1000\hat{\mathrm{M}}^{-1} = \begin{bmatrix} -0.087898618 & 0.1317748 & 0.1317748 & -0.0043706495 & 0 \\ 0.1317748 & -0.43244034 & -0.19376112 & 0.0065523381 & 0.018988844 \\ 0.1317748 & -0.19376112 & -0.43244034 & 0.0065523381 & -0.018988844 \\ -0.0043706495 & 0.0065523381 & 0.0065523381 & -0.092298356 & 0 \\ 0 & 0.018988844 & -0.018988844 & 0 & -0.095102461 \end{bmatrix} \tag{B.2}$$

$$\hat{h} = -0.000087898618 \tag{B.3}$$

These constant linearized values were arrived at by setting θ_1 and θ_2 to zero and calculating the resulting values of M, M^{-1} and h.
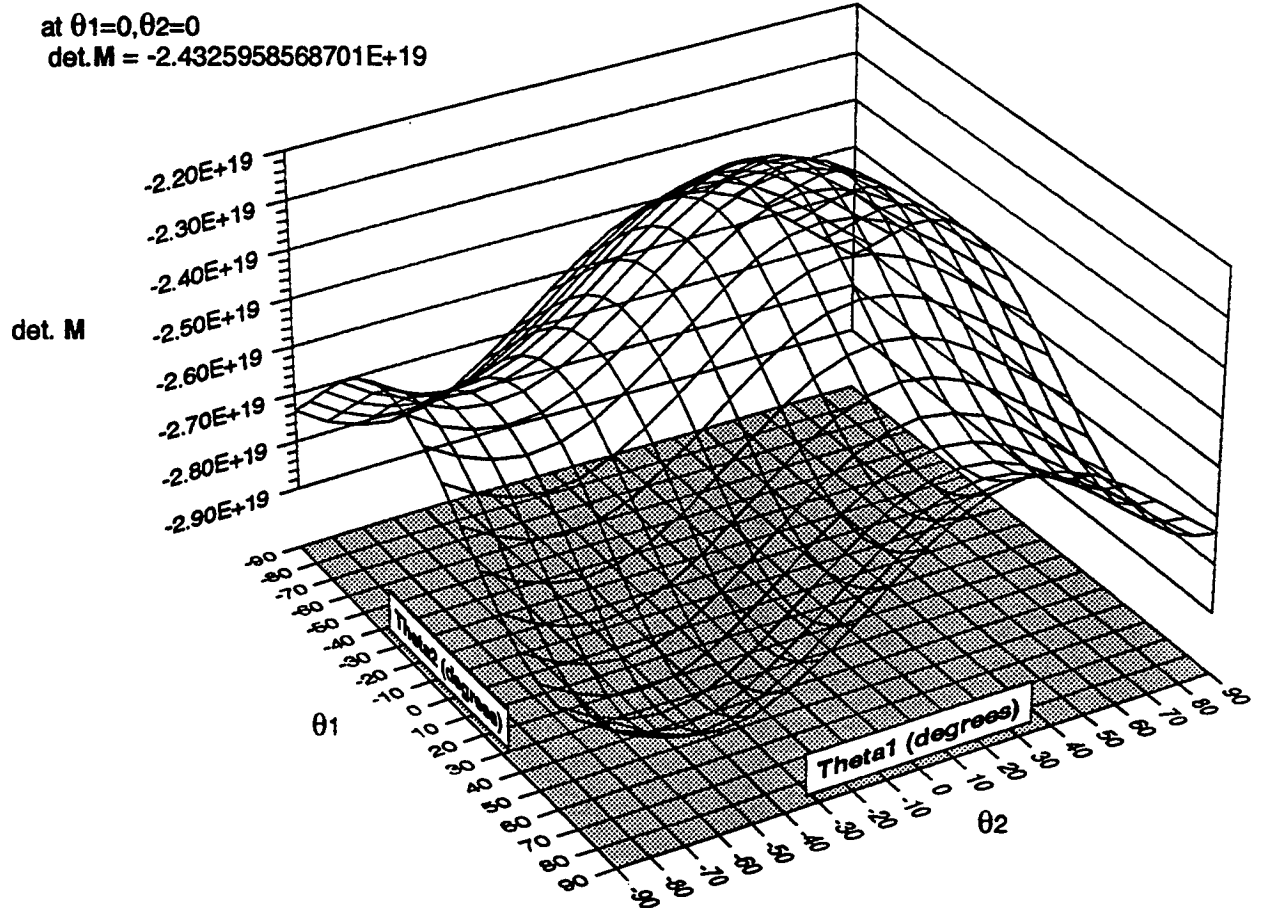
at $\theta 1=0, \theta 2=0$
det. M = -2.4325958568701E+19

Figure B-1: Variations in det. M

$\hat{h} = h = -0.000087898618$
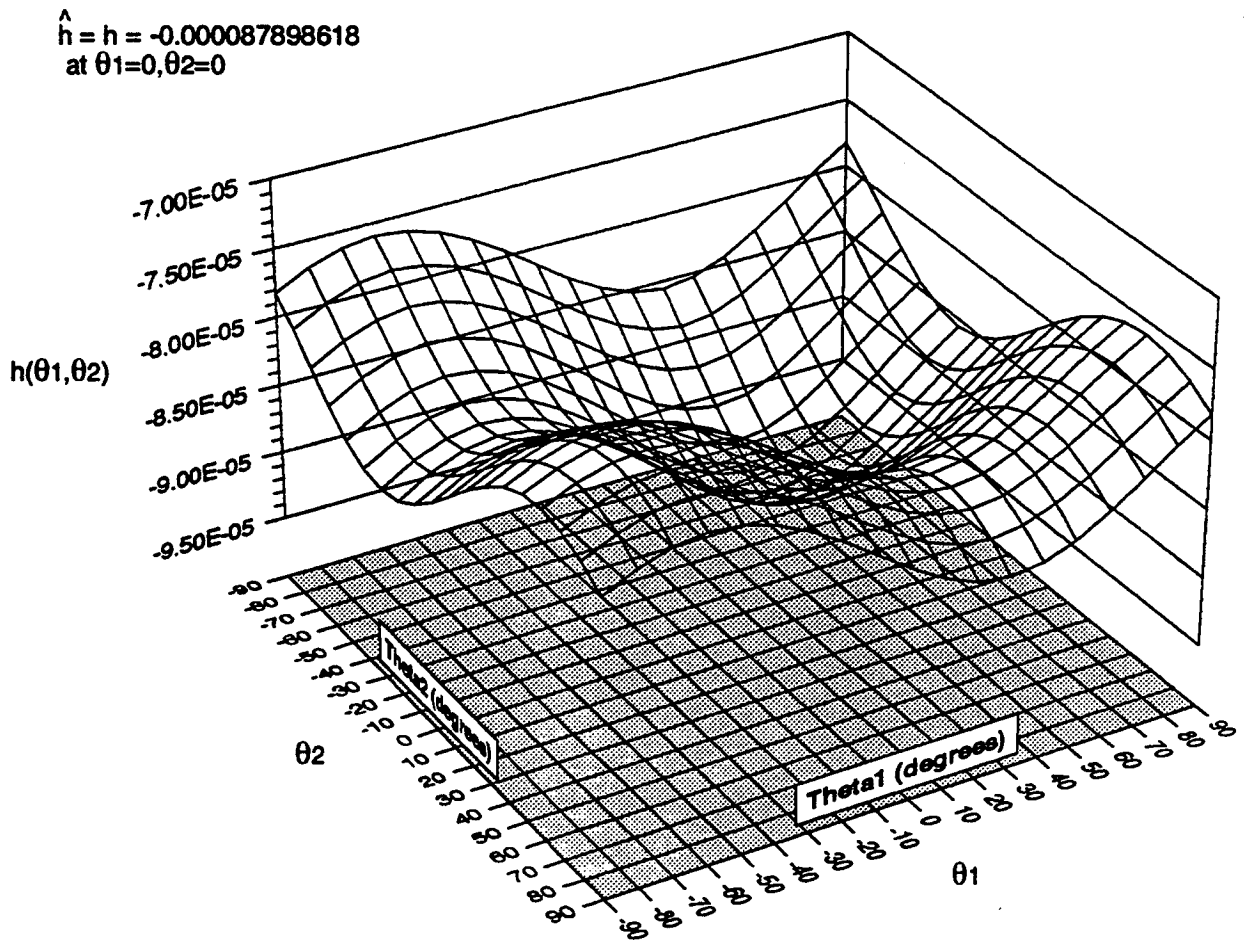at $\theta 1=0, \theta 2=0$

Figure B-2: Variations in h

APPENDIX C **DESIGN OF COMPOSITE PLANT/DISTURBANCE STATE-OBSERVERS FOR THE TI AND AD CONTROL MODES**

With the assumption that M is non-singular (a valid assumption as shown in App. B) then (A.6) can be rewritten as

$$\ddot{y} = -\mathrm{M}^{-1}\mathrm{D}\dot{y} - \mathrm{M}^{-1}\mathrm{K}y + \mathrm{M}^{-1}\mathbf{b}u + \mathrm{M}^{-1}f(y,\dot{y}) \tag{C.1}$$

DESIGN OF THE TI CONTROLLER GAINS. The equation for $\ddot{\phi}$ contained in (C.1) is

$$\ddot{\phi} = [\mathrm{M}^{-1}]_{1,1}u - g \tag{C.2}$$

where

$$
\begin{aligned}
g =& [\mathrm{M}^{-1}]_{1,2}(J_1 + l_1^2 M_1)(k_{11}\theta_1 + k_{12}\dot{\theta}_1) \\
&+ [\mathrm{M}^{-1}]_{1,3}(J_2 + l_2^2 M_2)(k_{21}\theta_2 + k_{22}\dot{\theta}_2) \\
&- \mathrm{M}^{-1}f(y,\dot{y})
\end{aligned}
\tag{C.3}
$$

The symbolic, analytical expressions for $[\mathrm{M}^{-1}]_{1,1}, [\mathrm{M}^{-1}]_{1,2}, [\mathrm{M}^{-1}]_{1,3}$ are extremely long and complicated and are not reproduced here. Linearizing this equation at $\theta_1 = \theta_2 = 0$ results in

$$\ddot{\phi} = \hat{h}u - \bar{g}(t) \tag{C.4}$$

where the $\bar{g}$ term includes the linearization error caused by the inevitable variation in M: that is,

$$\bar{g}(t) = g - ([\mathrm{M}^{-1}]_{1,1} - [\hat{\mathrm{M}}^{-1}]_{1,1})u \tag{C.5}$$

Next, we approximate the time-variation of $\bar{g}(t) \approx z_1$ by the m'th order polynomial spline (here $m = 1, 2, 3, \ldots$ is chosen by the designer).

$$\bar{g}(t) = c_1 + c_2 t + \ldots + c_m t^{m-1} \tag{C.6}$$

which implies that the dynamics of $\bar{g}(t)$ is modeled (approximately) by the m'th order system [3;p.413]

$$
\begin{bmatrix} \dot{z}_1 \\ \ddot{z}_1 \\ \vdots \\ \overset{(m)}{z}_1 \end{bmatrix}
=
\begin{bmatrix} 0 & \mathrm{I}_{m-1} \\ 0 & 0 \end{bmatrix}
\begin{bmatrix} z_1 \\ \dot{z}_1 \\ \vdots \\ \overset{(m-1)}{z}_1 \end{bmatrix}
+
\begin{bmatrix} \sigma_1(t) \\ \vdots \\ \sigma_{m-1}(t) \\ \sigma_m(t) \end{bmatrix}
\tag{C.7}
$$

where I_{m-1} is the $m-1$ order identity matrix and $\overset{(m)}{z}_1$ indicates the m'th derivative of z_1. The elements $\sigma_i(t)$ denote sparse sequences of randomly arriving, random intensity Dirac delta functions (impulses),

accounting for the once-in-a-while stepwise changes in the coefficients c_i of the approximating polynomial spline (C.6).

Utilizing the control separability property inherent in DAC design methodology [3;p.438] allows the HST control torque action, u, to be split into a set-point regulation part u_s and a disturbance cancellation part u_d as follows

$$u = u_s + u_d \tag{C.8}$$

where one defines u_s as

$$u_s = \hat{h}^{-1}\left(k_1\phi + k_2\dot{\phi}\right); \text{assuming } \phi_{sp} = 0 \tag{C.9}$$

and defines u_d as

$$u_d = \hat{h}^{-1}z_1 \tag{C.10}$$

Assuming $\bar{g}(t) \equiv \hat{z}_1; \hat{h} \approx h$, etc. the resulting closed-loop equation for ϕ is:

$$\ddot{\phi} + k_2\dot{\phi} + k_1\phi = 0 \tag{C.11}$$

where k_1 and k_2 can be chosen as in (8.b) to obtain the desired closed-loop dynamics for ϕ.

DESIGN OF THE TI OBSERVER GAINS. The composite equation of motion for (C.2),(C.5) and (C.7) is

$$
\begin{bmatrix} \dot{\phi} \\ \ddot{\phi} \\ \dot{z}_1 \\ \vdots \\ \overset{(m)}{z_1} \end{bmatrix}
=
\begin{bmatrix} 0 & \mathbf{I}_{m+1} \\ 0 & 0 \end{bmatrix}
\begin{bmatrix} \phi \\ \dot{\phi} \\ z_1 \\ \vdots \\ \overset{(m-1)}{z_1} \end{bmatrix}
+
\begin{bmatrix} 0 \\ [\hat{\mathbf{M}}]_{1,1}^{-1} \\ 0 \\ \vdots \\ 0 \end{bmatrix} u
+
\begin{bmatrix} 0 \\ 0 \\ \sigma_1(t) \\ \vdots \\ \sigma_m(t) \end{bmatrix}
\tag{C.12}
$$

Setting $\tilde{x} = \begin{bmatrix} \phi & \dot{\phi} & z_1 & \dots & \overset{(m-1)}{z_1} \end{bmatrix}^{\mathsf{T}}$, (C.12) can be written

$$\dot{\tilde{x}} = \tilde{\mathbf{A}}\tilde{x} + \tilde{b}u + \sigma \tag{C.13}$$

A full-order state-observer for (C.13) has the form

$$\dot{\hat{\tilde{x}}} = \tilde{\mathbf{A}}\hat{\tilde{x}} + \tilde{b}u + \mathbf{k}_o\mathbf{C}(\tilde{y} - \hat{\tilde{x}}) \tag{C.14}$$

where $(\hat{\cdot})$ denotes the observer's estimate of $(\cdot)$ and the plant output measurement is

$$\tilde{y} = C\tilde{x} = \phi \qquad (C.15)$$

The state-estimation error for the observer (C.14) is

$$\varepsilon = \tilde{x} - \hat{\tilde{x}} \qquad (C.16)$$

which obeys the well-known dynamical equation (between impulses of $\sigma(t)$)

$$\dot{\varepsilon} = (\tilde{A} - k_o C)\varepsilon \qquad (C.17)$$

where $k_o = [k_1, k_2, \ldots, k_{m+2}]^\mathsf{T}$.

Using (C.12), and assuming that the only output measurement is ϕ, the observer error dynamics (C.17) reduces to

$$\dot{\varepsilon} = \begin{bmatrix} -k_1 & & \\ \vdots & & I_{m+1} \\ -k_{m+1} & & \\ -k_{m+2} & 0 & \ldots & 0 \end{bmatrix} \varepsilon \qquad (C.18)$$

The characteristic polynomial of (C.18) is computed to be

$$s^{m+2} + k_1 s^{m+1} + \ldots + k_{m+1}s + k_{m+2} = 0 \qquad (C.19)$$

The roots of this polynomial may be set to any desired values via proper selection of the observer gains k_i.

If both ϕ and $\dot{\phi}$ are output measurements, the structure of the full-order observer (C.14) should be modified by setting $\tilde{y} = (\phi, \dot{\phi})^\mathsf{T}$ and redefining C accordingly, see [3;p.430].

DESIGN OF THE AD MODE CONTROLLER. We set $\tilde{D} = M^{-1}D$, $\tilde{K} = M^{-1}K$, $\tilde{f} = M^{-1}f(y,\dot{y})$, and define the state vector $\tilde{x}$ as

$$\tilde{x} = \begin{bmatrix} \phi, & \theta_1, & \theta_2, & \dot{\phi}, & \dot{\theta}_1, & \dot{\theta}_2 \end{bmatrix}^\mathsf{T} \qquad (C.20)$$

Then, owing to the form of the D and K matrices, the state vector equation of motion governing $\tilde{x}(t)$ becomes

$$\dot{\tilde{x}} = A\tilde{x} + \tilde{b}u + \tilde{\omega} \qquad (C.21)$$

where

$$\theta = (\theta_1 + \theta_2)/\sqrt{2} \tag{C.26}$$

A COMPOSITE STATE-OBSERVER FOR THE AD MODE. A full-order state-observer for (C.22) has the form

$$\dot{\hat{\tilde{x}}} = \tilde{A}\hat{\tilde{x}} + \hat{\tilde{b}}u + k_o(\tilde{y} - C\hat{\tilde{x}}) \tag{C.27}$$

where $\hat{\tilde{x}}$ denotes the estimates of $\tilde{x}$ and the output measurements are denoted by

$$\tilde{y} = C\tilde{x} = \phi \tag{C.28}$$

The observer's state estimation error is defined by

$$\varepsilon = \tilde{x} - \hat{\tilde{x}} \tag{C.29}$$

which has the error dynamics:

$$\dot{\varepsilon} = (\bar{A} - k_o C)\varepsilon; \qquad k_o = [k_1, k_2, \ldots, k_6]^\top \tag{C.30}$$

Using the Linearized Model in Appendix C, and assuming that the only output measurement is $\phi(t)$, (C.30) reduces to

$$\dot{\varepsilon} = \begin{bmatrix} -k_1 & 0 & 0 & 1 & 0 & 0 \\ -k_2 & 0 & 0 & 0 & 1 & 0 \\ -k_3 & 0 & 0 & 0 & 0 & 1 \\ -k_4 & -[\tilde{K}]_{1,2} & -[\tilde{K}]_{1,3} & 0 & -[\tilde{D}]_{1,2} & -[\tilde{D}]_{1,3} \\ -k_5 & -[\tilde{K}]_{2,2} & -[\tilde{K}]_{2,3} & 0 & -[\tilde{D}]_{2,2} & -[\tilde{D}]_{2,3} \\ -k_6 & -[\tilde{K}]_{3,2} & -[\tilde{K}]_{3,3} & 0 & -[\tilde{D}]_{3,2} & -[\tilde{D}]_{3,3} \end{bmatrix} \varepsilon \tag{C.31}$$

The eigenvalues of (C.31) can now be chosen to obtain the desired observer dynamics and the corresponding k_o can be computed.

If both ϕ and $\dot{\phi}$ are output measurements the full order observer (C.27) should be reconfigured by setting $\tilde{y} = [\phi, \dot{\phi}]^\top$, modifying C accordingly, and proceeding as before.

Singular Case. As shown in Appen. D, the equation for computing the observer gain $\mathbf{K}_o$ becomes singular when $\mathbf{M}$ is symmetric, $k_{11} = k_{21}$ and $k_{12} = k_{22}$. In this case, disturbances caused by the Solar Arrays appear as a single disturbance with one dynamical characteristic. In that case the same observer design method outlined above is used but with the transformation of variable (C.24) and associated state reduction (C.26).

Appendix D CONTROLLABILITY AND OBSERVABILITY ANALYSIS FOR THE CASE OF DYNAMICALLY SYMMETRIC SOLAR ARRAYS

Observability Analysis. When the solar arrays in Fig. 2 are dynamically symmetric (i.e. $k_{11} = k_{21}$ and $k_{12} = k_{22}$). The linearized state equations (C.22) for ϕ, θ_1, and θ_2 result in a full-order observer equation of the form:

$$
\begin{aligned}
\dot{\hat{x}} &= \mathbf{A}_0 \hat{x} + \mathbf{b}_0 u + \mathbf{k}_o (y - \hat{x}); \\
x &= \begin{bmatrix} \phi & \theta_1 & \theta_2 & \dot{\phi} & \dot{\theta}_1 & \dot{\theta}_2 \end{bmatrix}^\mathsf{T}; \\
y &= \mathbf{C}x = \phi
\end{aligned}
\tag{D.1}
$$

where

$$
\mathbf{A}_0 = \begin{bmatrix}
0 & 0 & 0 & 1 & 0 & 0 \\
0 & 0 & 0 & 0 & 1 & 0 \\
0 & 0 & 0 & 0 & 0 & 1 \\
0 & b & b & 0 & c & c \\
0 & d & e & 0 & f & g \\
0 & e & d & 0 & g & f
\end{bmatrix}; \qquad
\mathbf{b}_0 = \begin{bmatrix} 0 \\ 0 \\ 0 \\ 1 \\ 0 \\ 0 \end{bmatrix}
\tag{D.2}
$$

and

$$
\mathbf{k}_o = \begin{bmatrix} k_1 & k_2 & k_3 & k_4 & k_5 & k_6 \end{bmatrix}^\mathsf{T}
\tag{D.3}
$$

Assuming that $y = \mathbf{C}x = \phi$ and defining the observer estimation error for (D.1) to be

$$
\varepsilon = x - \hat{x}
\tag{D.4}
$$

The dynamics of $\varepsilon(t)$ are governed by

$$
\dot{\varepsilon} = (\mathbf{A}_0 - \mathbf{k}_o \mathbf{C})\varepsilon
\tag{D.5}
$$

where

$$\mathbf{A}_0 - \mathbf{k}_o\mathbf{C} = \begin{bmatrix} -k_1 & 0 & 0 & 1 & 0 & 0 \\ -k_2 & 0 & 0 & 0 & 1 & 0 \\ -k_3 & 0 & 0 & 0 & 0 & 1 \\ -k_4 & b & b & 0 & c & c \\ -k_5 & d & e & 0 & f & g \\ -k_6 & e & d & 0 & g & f \end{bmatrix}$$

(D.6)

Equating $det\left[sI - (\mathbf{A}_0 - \mathbf{k}_o\mathbf{C})\right]$ to a general sixth order polynomial in s yields

$$det\left[sI - (\mathbf{A}_0 - \mathbf{k}_o\mathbf{C})\right] = s^6 + p_5 s^5 + p_4 s^4 + p_3 s^3 + p_2 s^2 + p_1 s + p_0$$

(D.7)

which allows the k_i's to be determined. The result is:

$$p_5 = -2f + k_1$$

$$p_4 = (-2d + f^2 - g^2) - 2fk_1 + k_4$$

$$p_3 = 2(df - eg) + (f^2 - 2d - g^2)k_1 + b(k_2 + k_3) - 2fk_4 + c(k_5 + k_6)$$

$$p_2 = (d^2 - e^2) + 2(df - eg)k_1 + (cd + ce - 2bf)(k_2 + k_3) + (f^2 - 2d - g^2)k_4$$
$$+ (b - cf + cg)(k_5 + k_6)$$

$$p_1 = (d^2 - e^2)k_1 + \left[b(e - d + f^2 - g^2) + c(g - f)(d + e)\right](k_2 + k_3) + 2(df - eg)k_4$$
$$+ \left[b(g - f) + c(e - d)\right](k_5 + k_6)$$

$$p_0 = \left[b(d - e)(f + g) + c(e^2 - d^2)\right](k_2 + k_3) + (d^2 - e^2)k_4 + b(e - d)(k_5 + k_6)$$

(D.8)

As shown above, the six equations for p_i have only four variables: k_1, $(k_2 + k_3)$, k_4, and $(k_5 + k_6)$. This is due to a loss of complete observability of the pair $(\mathbf{A}_0, \mathbf{C})$ when the solar array flex modes shown in Fig. 2 are dynamically symmetric. The observer gains are thus not generally solvable for the symmetric case. The set of equations (D.8) however does suggest that in the dynamically symmetric solar array case the original state $\hat{x}$ in (D.1) should be reduced in dimension to read $\bar{x} = [\phi, \quad (\theta_1 + \theta_2), \quad \dot{\phi}, \quad (\dot{\theta}_1 + \dot{\theta}_2)]$ which will restore complete observability to the reduced system.

Controllability Analysis. The controllability matrix for (C.22) in the case of symmetric solar arrays is

$$\begin{bmatrix} \mathbf{b}_0 & \mathbf{A}_0\mathbf{b}_0 & \mathbf{A}_0^2\mathbf{b}_0 & \mathbf{A}_0^3\mathbf{b}_0 & \mathbf{A}_0^4\mathbf{b}_0 & \mathbf{A}_0^5\mathbf{b}_0 \end{bmatrix} = \begin{bmatrix} 0 & 1 & 0 & 0 & 0 & 0 \\ 0 & 0 & 0 & 0 & 0 & 0 \\ 1 & 0 & 0 & 0 & 0 & 0 \\ 0 & 0 & 0 & 0 & 0 & 0 \\ 0 & 0 & 0 & 0 & 0 & 0 \\ 0 & 0 & 0 & 0 & 0 & 0 \end{bmatrix}$$

(D.9)

which obviously has rank=2 indicating that not all of the states of (C.22) are controllable when the two solar arrays are dynamically symmetric.

Chapter 2

FUNDAMENTAL CONCEPTS AND LIMITATIONS IN PRECISION POINTING AND TRACKING PROBLEMS

Chapter Summary

In this Chapter, we first describe the generic pointing and tracking problems in a general dynamical system/state-space context. Then, we analyze the information-theoretic aspects of the various uncertain signals in those problems, and establish some fundamental performance limitations those uncertainties induce, using various results and principles of modern control theory. It is shown that the introduction of "waveform models" for uncertain signals, leading to an extended-state formulation of pointing and tracking problems, is the most effective rational means of coping with those fundamental limitations.

1. *INTRODUCTION*

The design of pointing and tracking control systems constitutes one of the most important and widespread application areas for the field of control engineering. In spite of a long history of successful industrial applications, dating back at least to the early 1940's, the fundamental scientific/theoretical aspects of pointing and tracking control problems are still not well-understood owing to the uncertain nature of several features of those problems. In particular, the time-varying pointing/tracking commands associated with such problems are typically not known *a priori*, but are only revealed on-line, in a real-time manner. Moreover, the internal and external disturbances that degrade the performance of pointing and tracking control systems are

inherently uncertain in nature and typically cannot be directly measured in real-time. These uncertainty features induce subtle performance limitations to the "solutions" of pointing and tracking control problems. The scientific aspects of those limitations have received very little attention in the literature.

In this Chapter we examine the information-theoretic nature of the uncertainties inherent in pointing and tracking control problems, and identify the theoretical performance limitations induced by those uncertainties. It is shown that a novel "waveform model" representation of pointing/tracking commands, and of internal/external disturbance actions, offers the most effective rational means of coping with those inherent performance limitations.

2. POINTING AND TRACKING PROBLEMS; FUNDAMENTAL CONCEPTS

The scientific consideration of pointing and tracking control problems necessitates a precise description of the essential conceptual features of the class of pointing and tracking problems to be considered. For this purpose we propose the (abstract) definitions given below. In both definitions, the dynamical system S being controlled is understood to consist of some physical hardware device (i.e. electro-mechanical-optical, etc.) that has a known, reliable mathematical model, a finite-dimensional state vector $x=(x_1,\cdots,x_n)$, r distinct control inputs $u=(u_1,u_2,\cdots,u_r)$ (i.e. control motors, torquers, linear actuators, etc.) and p distinct disturbance inputs $\{w_1(t),w_2(t),...,w_p(t)\}$ (i.e. wind gusts, target motions, coulomb frictions, structural distortions, flex-body vibrations, etc.). The outputs $\{y_1,y_2,\cdots,y_m\}$ of S consists of those features of S (positions, rates, accelerations, etc.) that can be measured by available sensors, in real-time.

Definition of the Pointing Control Problem - For purposes of this Chapter, the pointing control problem for a dynamical system S is understood to consist of the analytical design of the vector $u(\cdot)$ of control inputs $u = (u_i, u_2, \cdots, u_r)$ such that each of certain designated outputs $y_i(t)$ of S is forced to promptly attain, and steadfastly *remain at*, a specified constant value (given set-point value) $y_{i,sp}$ in the face of an "arbitrary" initial-state $x(t_o)$ of S and any transient or persistent vector w of disturbance-actions $w(t) = \big(w_1(t), w_2(t), \cdots, w_p(t)\big)$ that are likely to act on S. Generally speaking, the "constant" set-point values $y_{i,sp}$ may abruptly change to some new constant value from time-to-time in an unknown, stepwise-constant manner.

There are, of course, special applications of pointing control systems where it is required to "point" $y_i(t)$ at one and only one, specific set-point $y_{i,sp}$, and therefore sudden, unexpected jumps in $y_{i,sp}$ do not occur. To maintain the generality of our comments and characterizations we will hereafter disregard such special, restricted cases.

Definition of the Tracking Control Problem - The tracking control problem for S consists of the analytical design of the vector of control inputs $u = (u_i, u_2, \cdots, u_r)$ such that each one of certain designated outputs $y_i(t)$ of S is forced to promptly coincide-with and thereafter faithfully follow (track with high-fidelity) an associated time-varying command input $y_{i,c}(t)$, in the face of an "arbitrary" initial-state $x(t_o)$ of S and any transient or persistent vector $w(t)$ of disturbance actions $w(t) = \big(w_1(t), w_2(t), \cdots, w_p(t)\big)$ that are likely to act on S.

It is clear from these definitions that the general pointing problem is a special case of the tracking problem in which the time-varying "tracking-commands" $y_{i,c}(t)$ become constant (set-point) commands $y_{i,sp}$.

3. FUNDAMENTAL LIMITATIONS IN POINTING AND TRACKING PROBLEMS: INFORMATION-THEORETIC ISSUES

The primary sources of uncertainty, in the pointing and tracking problems defined above, lie in: (i) the ways the set-point/tracking commands $\{y_{i,sp}(t)$, $y_{i,c}(t)\}$ and the disturbance inputs $\{w_j(t)\}$ naturally evolve in time and (ii) the way in which a pointing/tracking control system becomes aware of, and responds to, set-point/tracking commands and to the presence and nature of a disturbance input $w_j(t)$.

3.1 *Time-Evolution of Pointing/Tracking Commands*

In regard to the time-evolution of the set-point/tracking commands, it is typically the case that the time-behavior of $\{y_{i,sp}(t), y_{i,c}(t)\}$, are not known to the control designer *a priori*. Moreover, the values of $y_{i,sp}(t)$ and $y_{i,c}(t)$ at time t are not known to the controller until time t. In fact, the underlying exogenous physical processes that determine how $y_{i,sp}(t)$ and $y_{i,c}(t)$ evolve in time are typically such that at time t the future behavior of $y_{i,sp}(\tau)$, $y_{i,c}(\tau)$, $\tau > t$, is not only not known, it is not determinable! This latter fact is rather subtle and warrants further elaboration. Some typical time-plots of set-point and tracking commands, representing an after-the-fact recording of data, are shown in Figure 1. The distinguishing feature of each plot, from our perspective, is that $y_{i,sp}(t)$ and $y_{i,c}(t)$ have a smooth, well-behaved waveform pattern (trace) except at a few isolated random-like "transition times" t_i where an abrupt change occurs in either the value of ($y_{i,sp}(t)$, $y_{i,c}(t)$) and/or the value of some derivative of $y_{i,c}(t)$. Between any two successive transition times t_i, t_{i+1} the plot of $y_{i,c}(t)$ continues to be smooth and well-behaved, although not necessarily exhibiting the same pattern of behavior between each such pair of transition times.
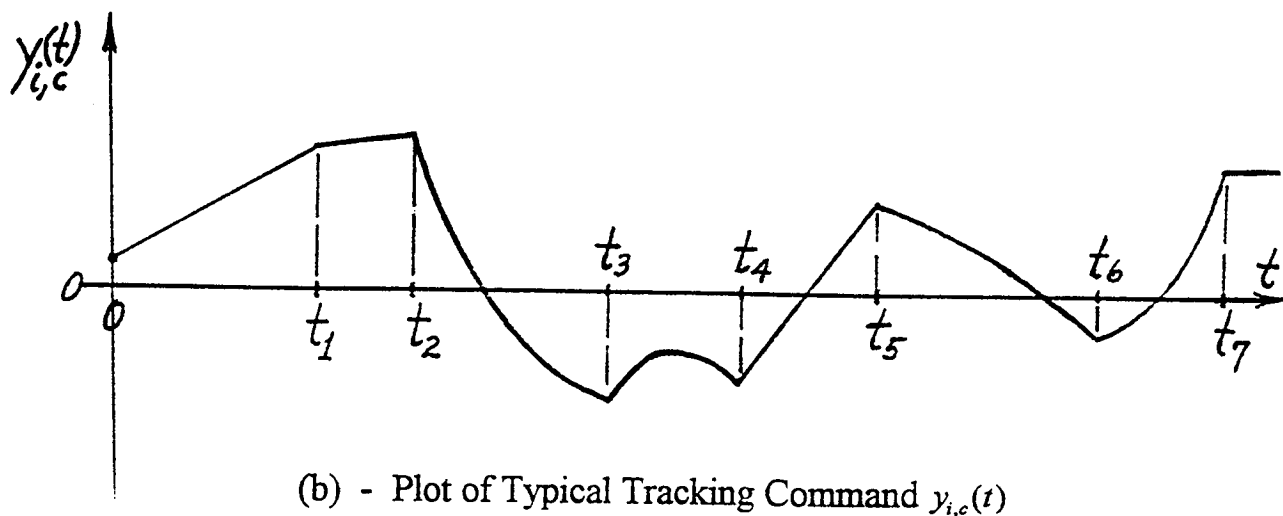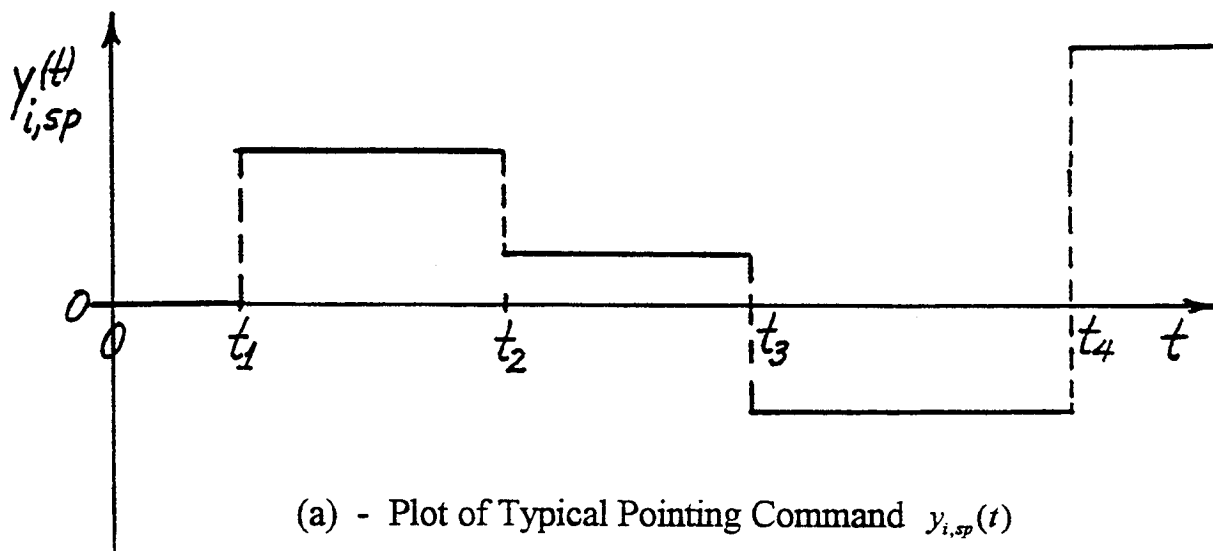
(a) - Plot of Typical Pointing Command $y_{i,sp}(t)$

(b) - Plot of Typical Tracking Command $y_{i,c}(t)$

Figure 1 - Plot of Typical Pointing/Tracking Commands $y_{i,sp}(t)$, $y_{i,c}(t)$

If $y_{i,sp}(t_i + \varepsilon)$ is known, for a sufficiently small $\varepsilon > 0$ then clearly the behavior of a set-point command $y_{i,sp}(t)$ is accurately predictable between any two successive transition-times t_i, t_{i+1} . However, this seemingly deterministic character of $y_{i,sp}(t)$ is deceiving because the transition times $t_i, t_{i+1} \cdots$ *themselves* are determined by complex exogenous factors that are (typically) *not* quantifiable, *a priori*, and thus are inherently unknown, unpredictable and, in fact, are indeterminable, *a priori*. Therefore it is (typically) impossible to know or predict $y_{i,sp}(t)$ beyond the (unknown) "next" transition time t_{i+1} .

A similar remark applies to tracking commands $y_{i,c}(t)$. Between any two successive transition times t_i, t_{i+1} the behavior of $y_{i,c}(t)$ is conceptually predictable, at least over short sub-intervals of (t_i, t_{i+1}) , from knowledge of an initial record of $y_{i,c}(\tau)$ over a small interval $t_i < \tau \le (t_i + \varepsilon), \varepsilon = $ small >0, since $y_{i,c}(t)$ and its' derivatives $d^k y_{i,c}(t)/dt^k, k = 1,2,\cdots$, are all continuous in the open interval $t_i < t < t_{i+1}$. For instance, in that case one can argue that at each t a Taylor-series expansion of $y_{i,c}(t)$ should yield a non-zero sub-interval of convergence within the interval $t_i < t < t_{i+1}$.

The foregoing observations lead us to postulate the following prototype characterization of the class of realistic pointing commands $y_{i,sp}(t)$ and tracking commands $y_{i,c}(t)$ most often encountered in industrial applications.

Prototype Characterization of Typical Pointing and Tracking Commands - The time-histories of typical pointing and tracking commands, illustrated in Figure 1, are characterized by a finite number of sequential, open, (not necessarily even), unknown intervals of time $t_i < t < t_{i+1}$, $i = 0,1,2,\cdots$, within which the functions $y_{i,sp}(t)$, $y_{i,c}(t)$ and their derivatives, vary in a

smooth, well-defined manner. At the (unknown) times $t = (\ t_i, t_{i+1}\ )$ the values of the functions $y_{i,sp}(t), y_{i,c}(t)$, and/or one or more of their time-derivatives, experience simple jumps whose values are unknown and unpredictable, *a priori*.

There are, undoubtedly, some exceptional cases one can cite in which it can be argued that this prototype characterization is not appropriate. However, we feel confident that this characterization <u>is</u> appropriate for the vast majority of real-life industrial applications involving pointing and tracking commands.

Comparison with Random Process Characterizations - Some control engineers and signal-processing specialists, tend to view any signal that is <u>not</u> completely determinable (and completely known) as a "random" signal that can only be characterized by its (long-term) mean-value, variance, and other (higher) moments, as used in random process theories. Thus it is instructive to compare our prototype characterization of typical pointing and tracking commands given above to the stochastic characterization of random processes.

The conceptual "signals" referred to in random-process theories as "white-noise" or "colored white-noise" [1] are mathematical constructs involving fictitious signals whose "values" go from "$+\infty$ to $-\infty$" on every (arbitrarily small) positive interval of time. In particular, the <u>Bode-Shannon realization</u> of mathematical white noise consists of a densely populated time-sequence of Dirac-impulses having completely random arrival times and intensities, where the time-interval Δt between any two successive impulse arrivals is <u>arbitrarily small</u>. Clearly, such a "signal" cannot have any waveform characteristics and, in fact, cannot exist physically. Moreover, if

such a signal is imagined to be fed into (input into) a physically existing linear dynamical system (a linear "coloring filter") the output response $y(t)$ of that system (called "colored noise") will be devoid of any distinguishable waveform characteristics, since then some higher derivative of $y(t)$ will always involve a "white noise" component. For instance, if one imagines the "coloring filter" to consist simply of a <u>pure integrator</u> so that

$$y(t) = \int_{t_o}^{t} (white\ noise) d\tau$$

the response $y(t)$ [called a Brownian or Wiener process] has no discernible waveform characteristics because its (formal) "derivative" dy/dt is a densely populated sequence of randomly-arriving, random-intensity impulses (i.e. white-noise).

It follows from these remarks that if, in the design of a tracking control system, the uncertain tracking commands $y_{i,c}(t)$ are viewed (mathematically modeled) as "white-noise", or some colored hue of white-noise, the possibility of the design process accommodating any inherent waveform patterns that may characterize the <u>actual</u> physical commands $y_{i,c}(t)$ is lost forever. In particular, if one only models or specifies the long-term average statistical mean and variance (or power-spectral density) of $y_{i,c}(t)$ in designing a tracking control system, one is (over)designing for an imagined class of commands $\{y_{i,c}(t)\}$ that includes outrageously rough, wildly-varying, *continuously un-differentiable* functions $y_{i,c}(t)$ that would never occur in the actual physical application. Moreover, the long-term average statistical characterizations of mean, variance, power-spectral density, of $y_{i,c}(t)$ etc. may be <u>completely irrelevant</u> to the required short-term tracking performance of, say, a missile seeker tracking a maneuvering target. Such short-term tracking performance requirements <u>demand</u> that the seeker control system

react to the instantaneous waveform-pattern behavior actually exhibited by the target motions at <u>each</u> moment of time t —and such real-time waveform behavior information is <u>never</u> reflected in the long-term averages of mean, variance, etc. of target motions. The latter consideration is a manifestation of the old statistical joke about a person drowning while crossing a wide, placid stream whose average depth is 2 cm.

In summary, high-performance tracking control systems operating in disturbance environments require real-time information about the <u>instantaneous</u> waveform characteristics of the particular tracking command $y_{i,c}(t)$, and of the particular disturbance input $w_j(t)$ acting at each moment of time t . Statistical characterizations of long-term average mean, variance, power-spectral density, etc. <u>do not</u> (and cannot) provide such real-time waveform behavior information about tracking commands and disturbances.

3.2 _Characterization of Disturbances_ - The various disturbances $w_j(t)$ that can act on the dynamical systems S involved in pointing and tracking control problems are almost always uncertain in nature and not accessible for direct measurement in real-time. Those disturbances arise from a variety of physical sources, some of which produce very erratic and capricious disturbance behavior. For example, fluid turbulence, radio-static, and similar "noisy" sources. Such disturbances have little, if any, discernible waveform characteristics and therefore, as a practical matter, can only be represented in terms of their averaged statistical properties. Thus, pointing and tracking control systems designed to cope with such noisy uncertain disturbances can only do so in a long-term averaged sense, such as <u>minimizing</u> the long-term average of the mean and/or the variance of the disturbance's effects on S . The design of such "good-on-the-average" controllers is addressed in the

subject of Stochastic Optimal Control Theory [2] and will not be further considered here.

Fortunately, the vast majority of uncertain disturbances $w_j(t)$ that arise in realistic pointing and tracking problems are associated with physical sources that are not "noisy" in the sense of the preceding paragraph. Some common examples of such uncertain disturbances are: coulomb friction and "stiction" effects, vibrations due to equipment motions, structural flexibility effects, out-of-balance and off-center effects, gyroscopic precession effects, gravity-gradient effects, crew motions, solar pressure effects, etc. In missile guidance problems the target's evasive maneuvers (jinking) appear as external "disturbances" in the guidance "error" equations. The time-history plots of such disturbances typically appear as shown in Figure 2, where it can be seen that, even though $w_j(t)$ is uncertain and unpredictable, the time behavior of $w_j(t)$ tends to be smooth and well-behaved except at a few isolated, randomly occurring moments of time t_i where the values of $w_j(t)$ and/or some of the higher time-derivatives $d^k w_j / dt^k$, $k = 1,2,3,\cdots$, experience simple random-like jumps. In other words, the inherent uncertainty of such disturbances does not prevent them from being characterized in terms of certain trends or patterns of waveform behavior they naturally tend to exhibit--between successive transition times (t_i, t_{i+1}) . This feature of disturbances $w_j(t)$ is recognized as being generically the same as that previously established for typical pointing and tracking commands; see Figure 1. Thus we are led to the following characterization.

Prototype Characterization of Typical Non-Noisy Disturbances in Pointing and Tracking Problems - The typical non-noisy disturbances $\{w_j(t)\}$ encountered in pointing and tracking problems are not known *a priori*, not
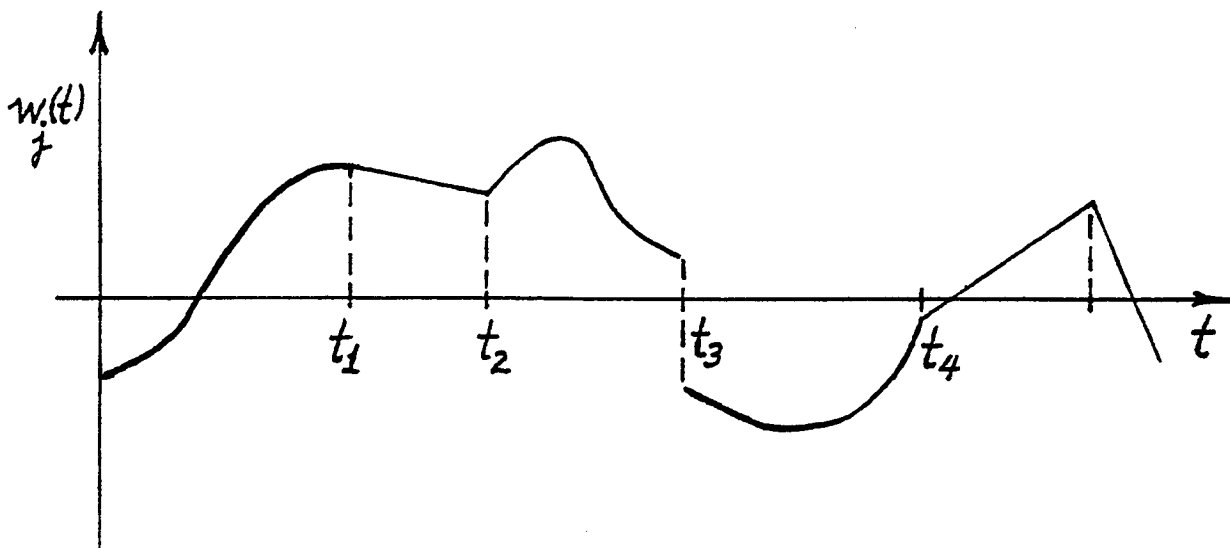
Figure 2 - Plot of Typical Disturbance Input $w_j(t)$

predictable, and not directly measurable. However the time behavior of each $w_j(t)$ is characterized by a sequence of unknown, finite, open time-intervals during which $w_j(t)$ and its derivatives are smooth, well-behaved functions of time. At the (unknown) ends of those time-intervals the value of $w_j(t)$, and/or certain of the higher time-derivatives of $w_j(t)$, experience unpredictable, simple, random-like jumps.

This completes our discussion of how typical set-point commands $y_{i,sp}(t)$, tracking commands $y_{i,c}(t)$ and disturbances $w_j(t)$ naturally evolve in time. In the next section we will examine the performance consequences of the particular way in which pointing/tracking control systems become aware of, and respond to, pointing/tracking commands and the presence of disturbances.

3.3 *Poincelle's Principle in Pointing and Tracking Control Problems* -
From the information-theoretic viewpoint, one of the primary contributors to performance limitations in pointing and tracking control problems is the fact that real-time changes which occur in the values of set-points or tracking commands at time t are not revealed to the control system until time t. Moreover, if some tracking command derivative $d^k y_{i,c}(t)/dt^k$, $k = 1,2,\cdots$, abruptly changes at time t, the tracking control system typically will not become fully aware of, and properly react to, that derivative change until some elapsed-time after t, (here we are disregarding the unusual case in which $y_{i,c}(t)$ and all of its time-derivatives can be accurately and directly measured in real-time). For example, if the value of $dy_{i,c}(t)/dt$ abruptly changes at time t, a "type-2" (double-integral) tracking control system will not become fully aware of, and properly react to, that derivative change until the resulting growth in the tracking error

$$e_i(t) = y_{i,c}(t) - y_i(t) \tag{1}$$

has persisted for some (small) time-interval. Consequently, a momentary build-up of tracking-error (1) is <u>necessary</u> to initiate the proper controller response in such a situation. A typical time-plot illustrating this behavior is shown in Figure 3.

The general fact that in a feedback control system some momentary build-up of error (1) is <u>necessary</u> to trigger the proper control response is known as Poincelle's Principle. This principle serves to establish a limit on the quality of tracking fidelity that can be achieved in tracking problems with realistic, uncertain tracking commands of the type we are considering here.

Poincelle's Principle also applies to the effect of uncertain, unmeasurable disturbances $w_j(t)$ associated with pointing and tracking problems. In particular, the only way a pointing/tracking control system can become aware of, and properly react to, the presence of such disturbances is by virtue of the system output deviations (response errors) caused by those disturbances. Thus, some momentary build-up of pointing/tracking error (1) is <u>necessary</u> to trigger the proper control response to an unknown, unmeasurable disturbance.

The only way one can overcome the pointing/tracking performance limitations imposed by Poincelle's Principle is for the controller to have <u>complete</u> *a priori* knowledge of <u>precisely</u> how the "future" pointing and tracking commands $\{y_{i,sp}(t), y_{i,c}(t)\}$ and disturbances $\{w_j(t)\}$ will vary with time, over the <u>entire</u> interval $t_o \le t \le T$ of the pointing/tracking control problem. We have already indicated that it is not realistic to expect such *a priori* information to be available in industrial pointing and tracking problems. However, it is interesting and instructive to consider how one
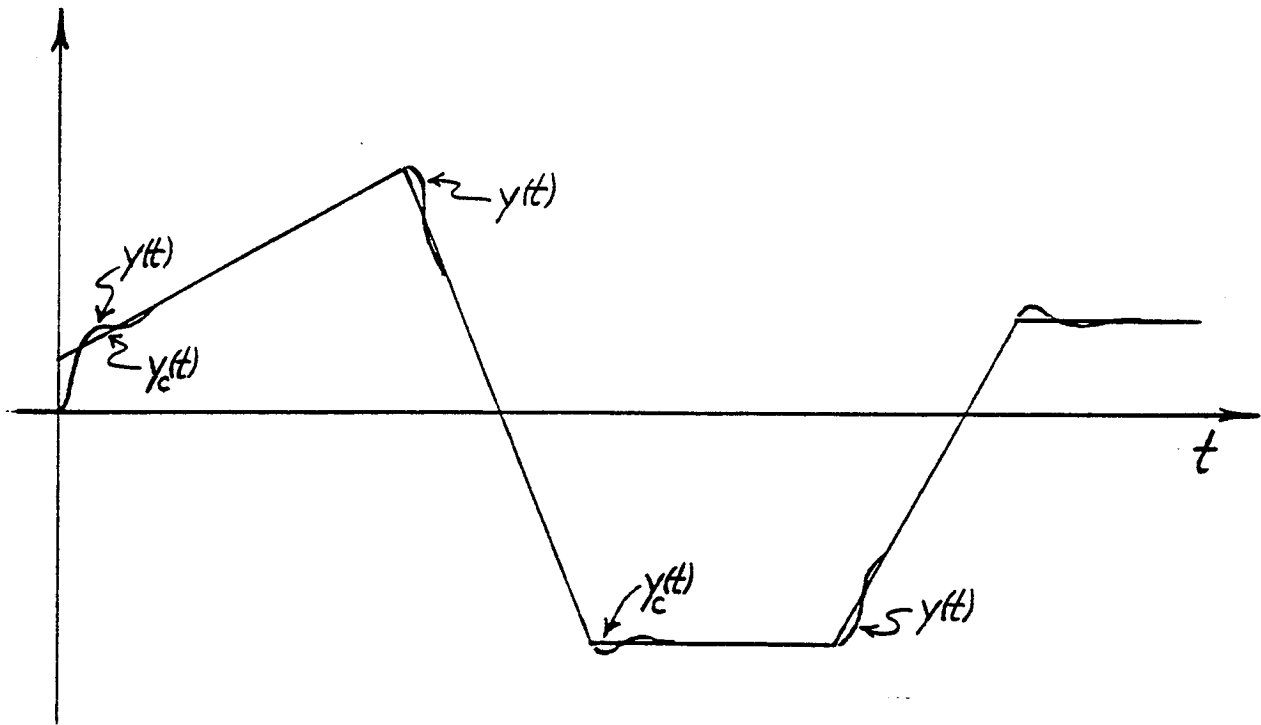
Figure 3 - Showing Momentary Build-Up of Tracking Error When
Derivative of Tracking Command Suddenly Changes

would design the "optimum" pointing/tracking control system for such an idealistic case. This subject is addressed in the next section.

4.0 *KALMAN'S THEORY FOR ABSOLUTE OPTIMAL CONTROL IN POINTING AND TRACKING PROBLEMS*

The performance limitations imposed by Poincelle's Principle are a fact-of-life in virtually all realistic pointing/tracking problems. Nevertheless, it is interesting to investigate (theoretically) the nature of the optimum control system, and the degree of enhanced performance that would accrue, if in the formulation of a pointing/tracking control problem one could hypothetically have complete *a priori* information on precisely how the pointing/tracking commands and disturbances will vary with time over the entire future interval of control. Such a hypothetical problem was posed and solved by Kalman in a highly original 1963 paper [3]. In this section, we will summarize the essential features of Kalman's problem formulation and solution.

4.1 *Kalman's Pointing/Tracking Problem* - The general pointing/tracking problem (called "servomechanism" problem) with disturbances, considered by Kalman in [3], was formulated for a very general class of multi-input/multi-output, possibly time-varying, linear dynamical systems S having the generic state-model [the symbols used below in (2) have been altered from those used in [3] to conform to current-day usage]

$$S: \quad \begin{cases} \dot{x} = A(t)x + B(t)u + F(t)w(t); \quad x(t_o) = x_o \\ y = C(t)x \end{cases} \quad (2a,b)$$

where $x = (x_1, \cdots, x_n)$, $u = (u_1, \cdots, u_r)$, $w = (w_1, \cdots, w_p)$ *and* $y = (y_1, \cdots, y_m)$. The overall pointing/tracking performance in Kalman's problem was measured by the (still popular) "error-quadratic/control-quadratic" performance criterion J defined by the functional

$$J[u] = e^T(T)Se(T) + \int_{t_o}^{T} [e^T(t)Q(t)e(t) + u^T(t)R(t)u(t)]dt \tag{3a}$$

$$e = (e_1, \cdots, e_m); \quad e_i \text{ -defined by (1),} \tag{3b}$$

where the error/control weighting matrices $\{S, Q, R\}$ are assumed symmetric and positive-definite for all t, and $[\ t_o, T\ ]$ denotes the specified time-interval over which the pointing/tracking control problem is defined. The problem is to find the control input $u = (u_1, \cdots, u_r)$ to the dynamic system (2) that _minimizes_ (3) for an _a priori_ known pointing/tracking command input

$$y_c(t) = (y_{1c}(t), \cdots, y_{m,c}(t)), \quad t_o \le t \le T \tag{4}$$

and an _a priori_ known disturbance input

$$w(t) = (w_1(t), \cdots, w_p(t)), \quad t_o \le t \le T. \tag{5}$$

4.2 _**Kalman's Solution**_ -   Kalman's solution to the optimum pointing/tracking control problem (2)-(5), with perfect knowledge of the "future," consists of the linear state-feedback control-law

$$u^o(t) = -R^{-1}(t)B^T(t)[P(t)x - h(t)] \tag{6a}$$

where the time-varying, symmetric positive-definite gain-matrix $P(t)$ and the vector $h(t)$ are determined, and stored for future use, by _reverse-time_ solution [i.e. integration from $t = T$ to $t = t_o$] of the following matric Riccati differential equation

$$\dot{P}(t) = -PA - A^TP + PBR^{-1}B^TP - C^TQC; \quad P(T) = C^TSC \tag{6b}$$

and the coupled vector-matric differential equation

$$\dot{h}(t) = (-A + BR^{-1}B^TP)^T h + PFw(t) - C^TQy_c(t); \quad h(T) = C^TSy_c(T). \tag{6c}$$

From our perspective, the most significant feature of Kalman's solution (6) is the fact that to carry-out the reverse-time solution of (6c), from $t = T$ to $t = t_o$, requires complete _a priori_ knowledge of $y_c(t)$ and $w(t)$, over $t_o \le t \le T$. In other words, _after_ integrating (6) in reverse-time, at each t in _forward-time_ playback (real-time use), the function $h(t)$ in the optimal control

law (6a) has <u>embodied in it</u> the optimal anticipatory control response that takes into account the (known) <u>entire future behavior</u> of $y_c(\tau)$ and $w(\tau)$, $t \leq \tau \leq T$. Thus, for example, if the tracking command or disturbance will have an abrupt jump in value at some "future time" $t_o < t_1 < T$, the "all knowing" optimal control $u^o(t)$ in (6) "knows" that fact at the time $t = t_o$ and will begin optimally reacting to that future jump <u>even before</u> the jump occurs! Accordingly, we will hereafter refer to (6) as the <u>absolute optimal control</u> for the pointing/tracking control problem (2)-(5).

The value of $J = J^o$ in (3) associated with a given initial state $x(t_o)$ of S in (2), and corresponding to use of the <u>absolute optimal</u> control (6) as the input to the dynamic system (2), is the <u>absolute minimal</u> value of J achievable by <u>any</u> pointing/tracking control system, assuming the same $x(t_o), y_c(t)$ *and* $w(t)$, $t_o \leq t \leq T$. Kalman showed, in [3], that J^o can be expressed as the sum of three terms:

$$J^o = x^T(t_o)P(t_o)x(t_o) - 2x^T(t_o)h(t_o) + \upsilon(t_o) \qquad (7a)$$

where the scalar $\upsilon(t)$ is computed by solving, in <u>reverse-time</u>, the auxiliary scalar differential equation

$$\dot{\upsilon}(t) = -y_c^T(t)Qy_c(t) + h^T(t)B(t)R^{-1}(t)B^T(t)h(t) + 2h^T(t)Fw(t); \qquad (7b)$$

with the "initial condition"

$$\upsilon(T) = y_c^T(T)Sy_c(T) \qquad (7c)$$

The availability of J^o enables one to explicitly compare the performance measure (3) for any practical pointing/tracking control system with the idealistic optimum performance (7a) hypothetically obtainable if one could have complete future knowledge of $y_c(t), w(t)$, *a priori*. In this way the fundamental performance limitations on (3), due to the practical <u>inability</u> to know the future behavior of $y_c(t)$ *and* $w(t)$, can be rigorously quantified and

precisely measured for any candidate, physically realizable pointing/tracking control system. Although Kalman's solution was developed for the specific quadratic-type performance measure (3), his solution methodology can be applied to other pointing/tracking performance measures J, with similar results and conclusions; see [4], [5].

4.3 _Apparent Failure of Bellman's Principle of Optimality_ - One of the cornerstones of modern optimal control theory for dynamical systems S is the assertion that the optimal control $u^o(t)$ at time t can always be expressed as a function of t and the system's state x at time t. In other words

$$u^o(t) = F(x(t), t) \quad , \ t_o \leq t \leq T. \tag{8}$$

for some unknown function $F(\cdot, \cdot)$ which is to be found by the analytical procedures of optimal control theory; see [6], [7].

Bellman popularized this assertion by elevating it to the status of a "principle" [8], which he called The Principle of Optimality. That principle can be paraphrased as follows: The optimal control at the present time t depends not on how the system S got into its present state $x(t)$, but only on t and the value of the present state $x(t)$ itself. In other words, the present state $x(t)$ embodies all of the "past" that is optimizationally relevant to determining the optimal control at the present time t.

A comparison of (6a) with (8) would seem to confirm Bellman's Principle of Optimality for the optimal pointing/tracking problem (2)-(5). However, when one realizes that the function $h(t)$ in (6a) cannot be determined from the "present" data ($x(t),t$), but rather must be determined from the future behavior of $y_c(\tau)$ and $w(\tau)$, $t \leq \tau \leq T$, it appears that the Principle of

Optimality fails in the case of pointing/tracking problems [note that the term $P(t)$ in (6a) does <u>not</u> induce this characteristic].

In the next section of this Chapter we will show how the introduction of <u>waveform-models,</u> and associated <u>state-models</u> for uncertain pointing/tracking commands $y_{i,c}(t)$ and uncertain disturbances $w_j(t)$ enables the <u>restoration of applicability</u> of the Principle of Optimality to pointing/tracking control problems—at the expense of a higher-dimension state-vector and some inevitable loss of performance compared to the hypothetical, idealistic absolute optimal performance (7a).

5. WAVEFORM-MODELS, STATE-MODELS, STATE-OBSERVERS AND A FUNDAMENTAL PRINCIPLE FOR ACCOMMODATING UNCERTAIN COMMANDS AND DISTURBANCES

The effective solution of pointing and tracking control problems has traditionally been hampered by the lack of mathematical models that can effectively represent the kind of (non-noisy) uncertain pointing/tracking commands and disturbances encountered in realistic applications, i.e. model the prototype characterizations of commands and disturbances given earlier in Sections 3.1 and 3.2. In this section we will describe a relatively new form of mathematical model that <u>is</u> effective in representing those prototype characterizations of uncertain commands and disturbances.

5.1 *Waveform Models* - The essential mathematical feature of the command and disturbance prototype characterizations given in Sections 3.1, 3.2 is that they are "analytic" between any two consecutive transition-times (t_i, t_{i+1}). An effective representation model of such functions is [here we use

the signal $y_{i,c}(t)$ to demonstrate the ideas involved; analogous results apply to $w_j(t)$]

$$y_{i,c}(t) = C_{i1}f_{i1}(t) + C_{i2}f_{i2}(t) + \cdots + C_{im_i}f_{im_i}(t) \qquad (9)$$

where the $\{C_{i1}, \cdots, C_{im_i}\}$ are <u>totally unknown</u> "constants" that are allowed to jump in value (at the transition times t_i) in an unknown, once-in-a-while manner as shown in Figure 4 and the $\{f_{i1}(t), f_{i2}(t), \cdots, f_{im_i}(t)\}$ are <u>completely known</u>, smooth, well-behaved, analytic time-functions called "basis functions." The representation (9) is a generalized "spline-model" for the uncertain signal $y_{i,c}(t)$ and can be compared to similar representations used across spatial domains in "finite-element" techniques [9]. In practice the basis functions $f_{i,j}(t)$ are chosen by the pointing/tracking designer to reflect the variety of waveform behavior patterns actually exhibited by typical commands $y_{i,c}(t)$. Thus, if the tracking command $y_{i,c}(t)$ typically looks like that shown in Figure 5 the corresponding spline-model (9) would be chosen as

$$y_{i,c}(t) = C_{i1} + C_{i2}e^{-3t} \quad ; \quad i.e. \quad f_{i1}(t) = 1; \quad f_{i2}(t) = e^{-3t} \qquad (10)$$

Likewise, if an uncertain disturbance $w_j(t)$ typically looks like that shown in Figure 6 its spline-model representation (9) would be chosen as

$$w_j(t) = C_{j1}e^{-2t}\sin(3t) + C_{j2}e^{-2t}\cos(3t) + C_{j3} \qquad (11a)$$

$$f_{j1}(t) = e^{-2t}\sin(3t) \; ; \; f_{j2}(t) = e^{-2t}\cos(3t) \; ; \; f_{j3}(t) = 1 \qquad (11b)$$

In some cases the typical waveform behavior of $y_{i,c}(t)$ (and/or $w_j(t)$) is simply an uncertain, irregular meandering back-and-forth motion as shown in Figure 7. For such cases, the appropriate representation (9) is a "polynomial-spline" of the form

$$y_{i,c}(t) = C_{i1} + C_{i2}t + C_{i3}t^2 + \cdots C_{im_i}t^{(m_i-1)} \qquad (12)$$
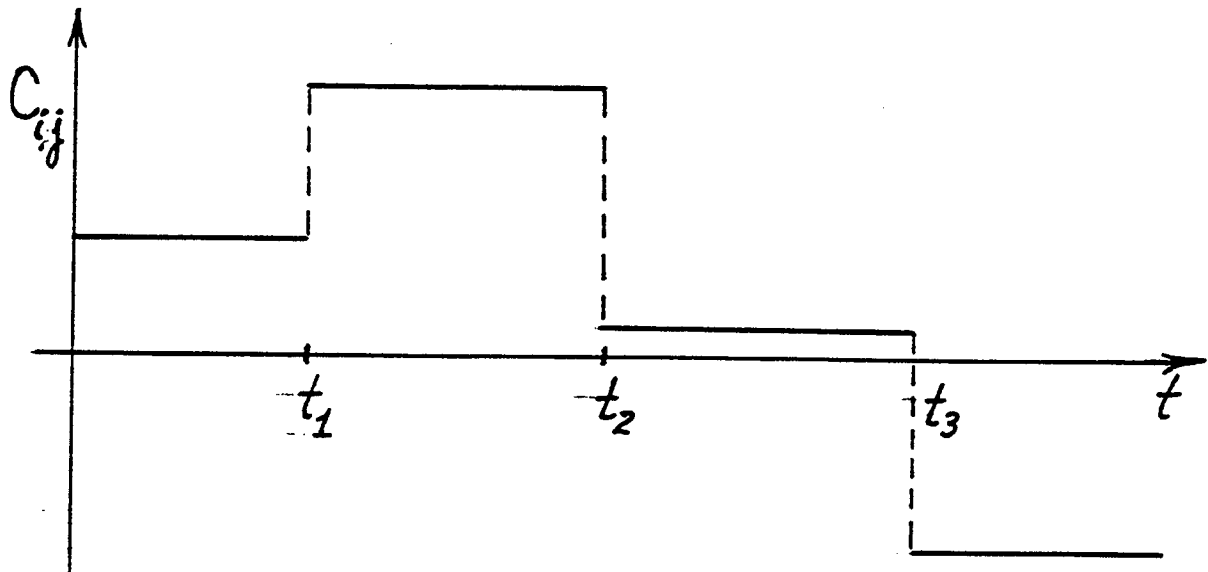
Figure 4 - Stepwise-Constant Behavior of Weighting
Coefficients C_{ij} in Waveform Model (9)

$y_{i,c}^{(t)}$

$\kappa \sim e^{-3t}$

$\kappa \sim e^{-3t}$

$\sim e^{-3t}$

t

Figure 5 - Plot of Tracking Command (10)

$w_j^c(t)$

$\sim e^{-2t} cos(3t)$

$\sim e^{-2t} cos(3t)$

t

Figure 6 - Plot of Disturbance (11a)

$y_{i,c}^{(t)}$

t

Figure 7 -   Plot of Uncertain Meandering Tracking Command that is
Appropriately Represented by the Polynomial Spline Model (12)

where the value of $m_i = 1, 2, 3, \cdots$ is chosen large enough to reflect the degree of back-and-forth motion exhibited by $y_{i,c}(t)$; typically $m_i \leq 4$ is satisfactory for industr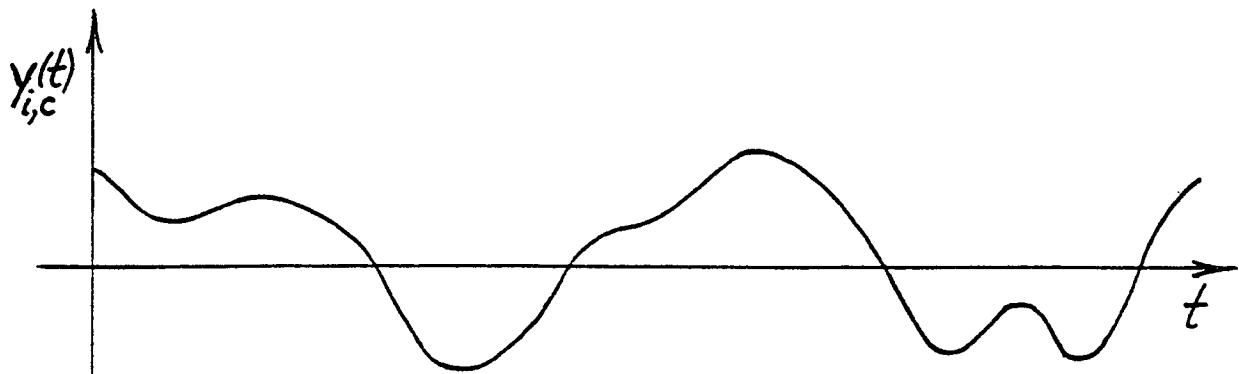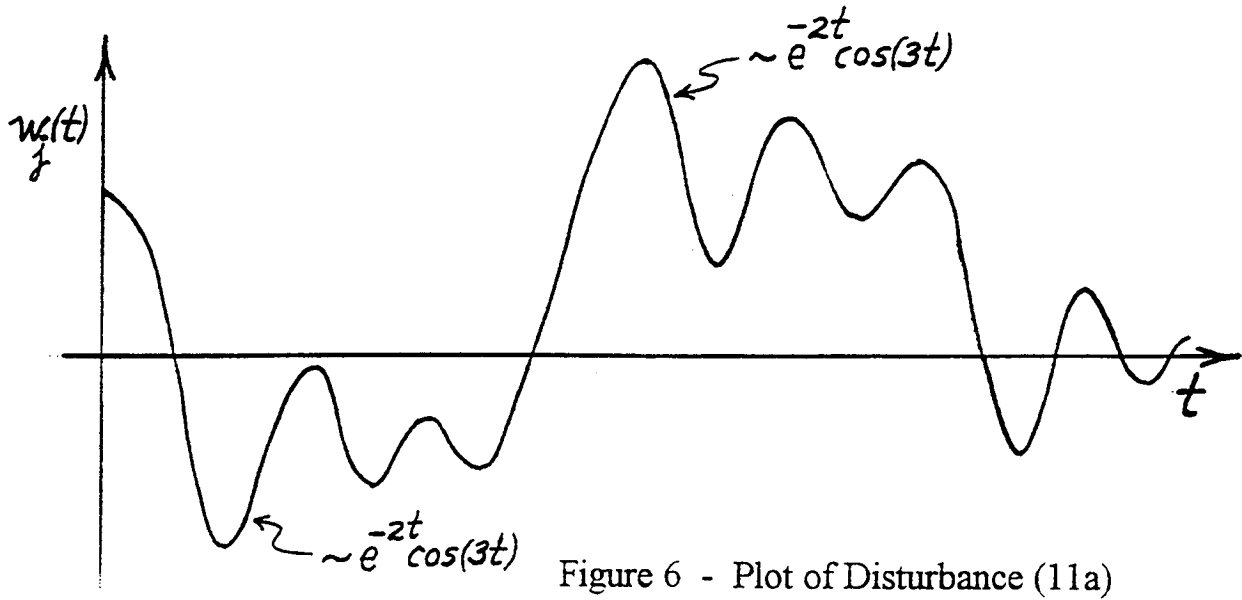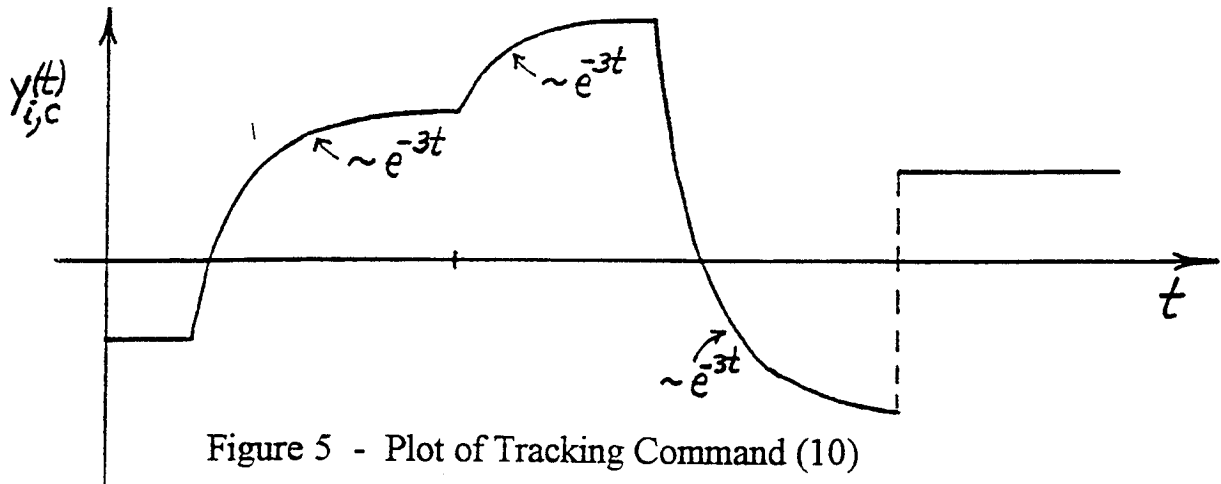ial applications. Note that the case $m_i = 1$ in (12) is the appropriate model for representing unknown, stepwise-constant pointing commands $y_{i,sp}(t)$. In (9)-(12) the unknown jumping of the "constants" C_{ij} at the (unknown) transition times t_i serves to represent the unknown jumping of $y_{i,c}(t)$, $w_j(t)$, and/or some of their time-derivatives, at those times.

Tracking commands and disturbances that admit a representation of the type (9) are said to posses "waveform-structure," and the representation (9) itself is known as a "waveform model." These concepts were introduced into the design of high-performance "disturbance control" systems in a series of papers beginning in 1968 [10]-[15]. The "information" encoded into the waveform model (9) is clearly non-statistical and is precisely the kind of dynamic, real-time command/disturbance waveform information needed in a pointing/tracking control problem to achieve maximum, physically realizable performance.

5.2 *Dynamic Models* - In order for a pointing/tracking controller to access the information encoded into (9) it is necessary to re-format that information by converting the waveform-model (9) to an associated "dynamic-model", which is simply a homogeneous differential equation that (9) satisfies (for strictly constant, non-zero C_{ij}). For this purpose one should seek the lowest-order of such an equation and, for mathematical convenience, it is prudent to select the set of basis functions $\{f_{ij}(t)\}$ in (9) from among those that satisfy some linear (possibly time-varying) differential equation. Actually, it turns-out that for industrial applications it is usually adequate to choose basis

functions $f_{ij}(t)$ in (9) that satisfy a <u>constant-coefficient linear differential</u> <u>equation</u>. In the latter case one obtains a "dynamic-model" for (9) in the form

$$d^{v_i}y_{i,c}(t)/dt^{v_i} + \beta_{v_i}d^{v_i-1}y_{i,c}(t)/dt^{v_i-1} + \cdots + \beta_2 dy_{i,c}(t)/dt + \beta_1 y_{i,c}(t) = 0 \qquad (13)$$

where the constant coefficients $\{\beta_1, \beta_2, \cdots, \beta_{v_i}\}$, and the order "$v_i$" of (13), are completely <u>independent</u> of the C_{ij} in (9) and are <u>precisely determined</u> by the chosen basis-functions $\{f_{i1}(t), \cdots, f_{im_i}(t)\}$ in (9). For example, in the case of (10) the associated dynamic-model (13) is

$$\dddot{y}_{i,c} + 3\ddot{y}_{i,c} = 0 \quad ; \qquad (\dot{\,}) = d(\,)/dt \qquad (14)$$

In the case (11a) the dynamic-model (13) is

$$\dddot{w}_i + 4\ddot{w}_i + 13\dot{w}_i = 0 \qquad (15)$$

The polynomial-spline waveform-model (12) leads to the m_i^{th} order dynamic-model

$$d^{m_i}y_{i,c}(t)/dt^{m_i} = 0 \qquad (16)$$

It is remarked that in some cases of multi-variable <u>coordinated</u> tracking commands $y_c = (y_{ic}, \cdots, y_{mc})$ (or multi-variable interacting disturbances) it may turn-out that the dynamic-model analogous to (13) consists of a <u>coupled set</u> of differential equations of the type (14)-(16). Note that (14)-(16) do not allow for (account for) the permitted, random-like, unknown once-in-a-while jumping of the weighting "constants" C_{ij} in (10)-(12). This deficiency will be corrected in the next subsection by introducing (symbolically) sparse sequences of unknown Dirac impulses as forcing functions in the "state-models" corresponding to (14)-(16).

5.3 *State-Models* - The final step in converting (13) for use by a pointing/tracking control system consists of re-formatting each of (13) into an equivalent set of first-order (state-variable type) differential equations. Thus, for instance, by defining the "tracking command state-variables" for each

independent $y_{i,c}(t)$ as:

<u>Command State-Variables</u> $c^{(i)} = (c_{i,1}, \cdots, c_{i,v_i})$

$$c_{i,1} = y_{i,c}; \quad c_{i,2} = \dot{y}_{i,c} ; \cdots c_{i,v_i} = \overset{(v_i-1)}{y_{i,c}} \qquad (17)$$

the most general state-variable equation for a set of possibly coupled dynamic equations of the type (13) can be written as [12; p. 640]

$$y_c = [G](c) \qquad ; \qquad c = col.(c^{(1)} | \cdots | c^{(m)}) = col.(c_1, \cdots, c_v); \quad v = \overset{m}{\underset{1}{\sum}} v_i \qquad (18a)$$

$$(\dot{c}) = [E](c) + \mu(t) \quad ; \qquad \mu = col.(\mu_1, \cdots, \mu_v) \qquad (18b)$$

where (G,E) are, respectively, $m \times v$ and $v \times v$ matrices that can be chosen from a family of canonical, completely observable pairs; see [12; p. 643]. The $\mu_i(t)$ in (18b) denote sparse sequences of unknown Dirac impulses that account for the random, once-in-a-while jumps that may occur in the C_{ij} in (9). In a like manner, one can define "disturbance state-variables" for each independent $w_j(t)$ as:

<u>Disturbance State-Variables</u> $z^{(i)} = (z_{i,1}, \cdots, z_{i,\rho_i})$

$$z_{i,1} = w_i \; ; \qquad z_{i,2} = \dot{w}_i \; ; \cdots ; z_{i,\rho_i} = \overset{(\rho_i-1)}{w_i} \qquad (19)$$

to obtain the following general state-variable equation for a set of (possibly coupled or coordinated) multi-variable disturbances $w = (w_1, \cdots, w_p)$

$$(w) = [H](z) \; ; \qquad z = col.(z^{(1)} | \cdots | z^{(p)}) = col.(z_1, \cdots, z_\rho); \quad \rho = \overset{p}{\underset{1}{\sum}} \rho_i \qquad (20a)$$

$$(\dot{z}) = [D](z) + \sigma(t) \; ; \qquad \sigma = col.(\sigma_1, \cdots, \sigma_\rho) \qquad (20b)$$

where, as in (18), the pair of matrices (H,D) can be chosen from a family of canonical, completely-observable pairs as explained in [13; pp. 405, 417] and the $\sigma_i(t)$ in (20b) denote sparse sequences of unknown Dirac impulses that account for the random, once-in-a-while jumping of the C_{ij} that may occur in the disturbance counterpart of expression (9), corresponding to the waveform model of $w_j(t)$. A more general version of (20) is given later in (32).

The particular choices (17), (19) of command and disturbance state-

variables are the most natural and convenient choices. However, as is well-known in the "state-theory" for dynamical systems, there are many other choices for state-variables that are equally valid [16; p. 170]—and some that are $\underline{not}$ valid; see [17]-[20]. The basis functions $\{f_{i,j}\}$, corresponding to the waveform models of $y_{i,c}(t)$, $w_j(t)$ appear in (18), (19) as the eigenmodes of the matrices E,D respectfully. For instance, in the case of m independent stepwise-constant pointing commands $y_{i,sp}(t)$, which have only the $\underline{one}$ basis-function $f_{i,1}(t) = 1$ $\underline{each}$, one obtains $E = O$, $G = I$, $\upsilon = m$ in (18). Note that it is $\underline{not}$ required that (E, D) be stable in order that (18), (20) model realistic commands and disturbances; i.e., see (12), (16).

It should be emphasized that, with the exception of the unknown, sparse, (symbolic) impulse-sequences $\mu(t)$, $\sigma(t)$ that have been added, the state-models (18), (20) are precisely the same as (and contain precisely the same "information" as) the dynamic model (13) and the disturbance counterpart of (13) (not shown). The virtue of the alternative format (18), (20) lies in the $\underline{explicit}$ recognition of $y_{i,c}(t)$, $w_j(t)$, and their time-derivatives, as individual, independent state-variables $\{c_{i,j}, z_{i,j}\}$ and in the fact that the existing theory of "state-observers" [Kalman filters], which we will be using in the sequel to estimate those state-variables in real-time, is formulated for general state-variable models of the type (18), (20). The assumption that the unknown impulse sequences $\mu_i(t)$, $\sigma_i(t)$ in (18), (20) are $\underline{sparsely}$ $\underline{populated}$ is critical to the existence of waveform structure for $y_{i,c}(t)$ and $w_j(t)$, respectively. In particular, as the impulses in the sequences $\mu_i(t)$, $\sigma_i(t)$ become more $\underline{densely}$ $\underline{populated}$ (time-spacing between successive impulse arrivals approaches zero) the sequences $\mu_i(t)$, $\sigma_i(t)$ begin to behave like the Bode-Shannon "white-noise" described in Section 3.1 with the result that $y_{i,c}(t)$, $w_j(t)$ in (18),

(20) lose all their waveform structure and (in those cases where E,D in (18), (20) happen to be stable matrices) begin to behave like conventional "colored-noises" of random process theory.

5.4 *A Fundamental Principle for Uncertainty Accommodation in Pointing/Tracking Control Problems* - The introduction in (17), (18) and in (19), (20) of the overall pointing/tracking command state $c = (c_1,c_2,\cdots,c_v)$ and overall disturbance state $z = (z_1,z_2,\cdots,z_p)$ is the key technical idea that allows practical realization of a pointing/tracking control system which achieves as near absolute optimal performance levels as is physically, rationally possible. This result, referred to as the Principle of Optimal Disturbance Accommodation in [4], can be re-stated for the class of pointing/tracking control problems considered here as follows.

> *The Command/Disturbance Uncertainty Accommodation Principle for Pointing/Tracking Control Problems*
> Suppose the commands $\{y_{i,c}(t)\}$ and disturbances $\{w_j(t)\}$ have known waveform-structures and state models in the sense of (9), (18), (20). Then, for a broad class of pointing/tracking performance measures J, and given dynamic systems S, the current values of the "states" $\{x(t), c(t), z(t)\}$ embody sufficient real-time "information" about S and the uncertain dynamic behavior of $\{y_{i,c}(t)\}$ and $\{w_i(t)\}$ to allow a rational, physically realizable, scientific "optimal" choice for the real-time control input $u(t)$— even though the future behavior of $y_{i,c}(t)$, $w_j(t)$ is not predictable at the time t.

The rationale for this principle is as follows. The state models for $x(t), c(t), z(t)$ are entirely deterministic and known, except for the sparse sequences $\sigma_i(t), \mu_i(t)$ of unknown impulses which cause corresponding, once-in-a-while, jumps in $(c(t), z(t))$. Since the sparse random-like arrival-times and random-like intensities characterizing those impulse sequences are totally unknown (have no statistical structure), there is no rational, scientific method for anticipating, and reacting *a priori* to, their jump effect on $(c(t), z(t))$ in an optimization problem. Thus, the "optimum" physically realizable, rational control strategy for such a situation is to choose $u(t)$, at each t, to optimally react to the "current" values of $x(t), c(t), z(t)$ as if there will be no further jumps in $c(t), z(t)$ in the future. This policy is equivalent to ignoring the presence of the $\sigma_i(t), \mu_i(t)$ impulses altogether, and can be viewed as a pseudo-restoration of Bellman's Principle of Optimality for pointing/tracking problems, in the extended (x,c,z)-state space. Of course, the ignored future jumps that will invariably and repeatedly occur in $c(t), z(t)$ do, in fact, affect the absolute optimal choice of $u(t)$, at each t. Thus our "optimum" physically realizable, rational control strategy, based on current values of $x(t), c(t), z(t)$ only, does not preclude the possibility of attaining "better-than-optimal" [but never better than absolute optimal!] performance by non-rational methods such as by fortuitous guessing about [gambler's luck, speculating on] the future impulse arrival times and their intensities. However such gambling in function spaces carries high risks with low probabilities of success and is definitely not recommended for precision pointing and tracking problems.

The "command/disturbance uncertainty accommodation principle" forms the foundation for the practical design of a new class of high-performance pointing/tracking control systems which must cope with uncertain tracking

commands and disturbances having the prototype characterizations defined in sections 3.1, 3.2 and illustrated in Figs. 1-3. That design procedure will be outlined in Section 6. First, however, we need to indicate just how the states $x(t)$, $c(t)$ and $z(t)$ can be accurately estimated in real-time.

5.5 _**State-Observers (Kalman Filters) for Estimation of (x(t), c(t), z(t)) in**_ _**Real-Time**_ - According to the uncertainty accommodation principle for commands and disturbances, as stated in the previous section, optimal pointing/tracking control laws $u^o = \mathcal{F}(\cdots)$ should be sought in the extended-state feedback/feedforward format [compare with (8)]

$$u^o = \mathcal{F}(x(t), c(t), z(t), t). \tag{21}$$

Thus, in addition to designing the "optimal" function $\mathcal{F}(\cdots)$ in (21) it is necessary to develop a practical means of generating accurate estimates $\hat{x}(t), \hat{c}(t), \hat{z}(t)$ of the three state vectors $x(t), c(t), z(t)$, in real-time. Fortunately, an effective means for accomplishing this latter task is provided by the existing Kalman Filtering Theory in the form of what is generically called a "state-observer." In this section, we briefly summarize the methodology whereby such state-observers can be designed to produce accurate real-time estimates $\hat{x}(t), \hat{c}(t), \hat{z}(t)$. We will focus attention here on the simplified cases where the pointing/tracking commands $y_{i,sp}(t), y_{i,c}(t)$, and outputs $y_1, \cdots, y_m$ of S, can be measured with negligible "sensor-noise". Otherwise one should use state-observers based on the full Kalman Filtering Theory, [21].

**Observation of the Pointing Command State** $c = (c_1, c_2, \cdots, c_v)$ - As indicated near the end of section 5.3, the state-variables c_i corresponding to a given, stepwise-constant pointing command $y_{sp} = (y_{1,sp}, y_{2,sp}, \cdots, y_{m,sp})$ are m in number ($v = m$) and are defined simply as

$$c_1 = y_{1,sp} \quad ; \quad c_2 = y_{2,sp} \quad ; \cdots ; \quad c_m = y_{m,sp} \tag{22}$$

Thus, in the special case of stepwise-constant pointing-commands, no command-state observer is required because the direct real-time measurement of the m signals $y_{i,sp}(t)$ constitutes a direct, real-time "observation" (measurement) of the associated command state $c = (c_1, \cdots, c_m)$.

State-Observers for the Tracking Command State $c = (c_1, c_2, \cdots, c_v)$ —

Assuming that $y_c(t)$ is not a stepwise-constant command, as just discussed, and that an appropriate command state-model (18) has been developed, an accurate real-time estimate $\hat{c}(t)$ of the command state $c(t)$ can be generated [between arrivals of the μ_i-impulses in (18b)] from real-time measurements of the m-vector $y_c(t)$ by the following (continuous-time) data-processing algorithm (full-order state-observer)

$$\dot{\hat{c}}(t) = E\hat{c} - K_o[y_c(t) - G\hat{c}] \tag{23}$$

where the $v \times m$ "observer gain-matrix" K_o is chosen by the designer to assure prompt decay to zero of the state estimation error

$$\varepsilon_c(t) = c(t) - \hat{c}(t) \tag{24}$$

between successive arrivals of the unknown impulses $\mu_i(t)$ in (18b). It is easy to show that $\varepsilon_c(t)$ in (24) is governed by the homogeneous linear equation

$$\dot{\varepsilon}_c = [E + K_o G]\varepsilon_c \tag{25}$$

Thus, if E, G are constant, K_o should be designed as a constant matrix that places all eigenvalues $\lambda_{i,o}$ of $[E + K_o G]$ in (25) sufficiently deep in the left-half plane. Since the pair (E, G) is, by construction, "completely observable," the latter is a standard task (pole-assignment) in modern control theory, [16]. The case of non-constant E and/or G is treated in a similar manner; see [12; p. 641].

The full-order (v^{th}-order) state-observer (23) can be replaced by any one of a variety of reduced-order state-observers---with the expense of a

somewhat more complicated mathematical structure, compared to (23). One such observer, having the reduced-order ($\upsilon - m$), is described in [13; p. 487].

Composite State-Observers for Simultaneous Estimation of the System-State $x = (x_1, \cdots, x_n)$ *and Disturbance-State* $z = (z_1, \cdots, z_p)$ – Unlike the command-state $c(t)$, which can be estimated via (23) from direct real-time measurements of the tracking command $y_c(t)$, the disturbance-state $z(t)$ can (typically) only be estimated from measurements of the <u>outputs</u> $y_1(t), \cdots, y_m(t)$ of the system S being controlled, (i.e. one typically cannot directly measure $w(t)$ in (20)). If the equations of motion for the state $x(t)$ of S can be reliably "linearized" about some nominal operating point (or operating condition) of S, the states $(x(t), z(t))$ of <u>both</u> S and $w(t)$ can be simultaneously estimated in real-time by a (full-order) "composite state-observer" as follows.

Suppose the state $x(t) = (x_1(t), x_2(t), \cdots, x_n(t))$ of S is governed by the <u>known, linearized</u> state-variable equations

$$S_L : \begin{cases} \dot{x}(t) = A(t)x + B(t)u(t) + F(t)w(t) \\ y(t) = C(t)x \end{cases} \qquad (26a,b)$$

where $\{A(t), B(t), F(t), C(t)\}$ are known matrices, and assume that an appropriate disturbance state-model (20) has been developed. Then, by incorporating (20) into (26) one obtains the following "composite plant/disturbance state-model" (hereafter we omit the permissible argument (t) on A, B, F, C, H, D to simplify notation)

$$\begin{pmatrix} \dot{x} \\ \dot{z} \end{pmatrix} = \begin{bmatrix} A & FH \\ \hline O & D \end{bmatrix} \begin{pmatrix} x \\ z \end{pmatrix} + \begin{bmatrix} B \\ \hline O \end{bmatrix} u(t) + \begin{pmatrix} O \\ \hline \sigma(t) \end{pmatrix} \qquad (27a)$$

$$y = [C|O] \begin{pmatrix} x \\ z \end{pmatrix} \qquad (27b)$$

By defining $\bar{x} = col.(x|z)$, the model (27) can be re-written in the more compact notation

$$\dot{\tilde{x}} = \tilde{A}\tilde{x} + \tilde{B}u + \tilde{\sigma} \qquad (28a)$$

$$y = \tilde{C}\tilde{x} \qquad (28b)$$

where the meanings of $\tilde{A}, \tilde{B}, \tilde{C}, \tilde{\sigma}$ are clear from comparison of (28) with (27). A full-order [$(n+p)th$-order] state-observer for generating an accurate composite-state estimate $\hat{\tilde{x}} = col.(\hat{x}|\hat{z})$, between arrivals of the unknown $\sigma_i(t)$ impulses in (27a), is given by the continuous-time data-processing algorithm [13; p. 431], [22]

$$\dot{\hat{\tilde{x}}} = \tilde{A}\hat{\tilde{x}} + \tilde{B}u(t) - \tilde{K}_o[y - \tilde{C}\hat{\tilde{x}}]. \qquad (29)$$

The composite-state estimation error $\tilde{\varepsilon} = \tilde{x} - \hat{\tilde{x}}$ associated with (29) is governed by the linear homogeneous equation

$$\dot{\tilde{\varepsilon}} = [\tilde{A} + \tilde{K}_o\tilde{C}]\tilde{\varepsilon} \qquad (30)$$

and thus the observer gain-matrix $\tilde{K}_o$ in (29) should be designed so that $\tilde{\varepsilon}(t) \to 0$ promptly, between arrivals of the σ_i-impulses in (27a). The latter task necessitates that the composite pair $(\tilde{A}, \tilde{C})$ in (28) be "completely observable," [a technical condition that is typically satisfied in industrial applications but, strictly speaking, is <u>not</u> automatically guaranteed, even if both (A, C) and (D, H) are known to be, <u>individually</u>, completely observable]. The design of $\tilde{K}_o$ is otherwise a standard task in modern control, [22].

The state-observer algorithm (29) can easily be generalized to include: (i) systems S whose vector of outputs $y(t)$ in (20b) is a (linear) function of $u(t)$ and/or $w(t)$ of the form

$$y(t) = C(t)x + \bar{E}(t)u(t) + \bar{G}w(t) \qquad (31)$$

and/or, (ii) disturbance sources such that the dynamic behavior of $w(t)$ depends linearly on the system state $x(t)$ and control $u(t)$ as follows [compare with (20)]

$$w(t) = H(t)z + L(t)x \qquad (32a)$$

$$\dot{z} = D(t)z + M(t)x + N(t)u(t) + \sigma(t) \qquad (32b)$$

The case (31) can arise when the sensors, used to measure the system outputs $y_i(t)$, include "accelerometers." The case (32) can arise from "state dependent" disturbances. Generalizations such as (31), (32), including additional "noise" terms, are addressed in [13; pp. 423, 424], [22], [23] and [24].

In addition to (29), various forms of reduced-order, composite-state observers for (28) can also be used to generate real-time estimates $\hat{x}(t), \hat{z}(t)$. The details of one such observer are presented in [22]. When the measurements of the pointing/tracking commands $(y_{i,p}(t), y_{i,c}(t))$ and/or the system outputs $y_i(t)$ are corrupted with (additive) "sensor noise" the corresponding state-observers (Kalman Filters) have exactly the same form as (23), (29) with the exception that the observer gain-matrices $(K_o, \bar{K}_o)$ in (23), (29), are then "optimally" determined by the (assumed known) noise statistics and by certain auxiliary equations (Riccati differential equations) as defined in Kalman Filtering Theory, [21].

In summary, when measurement noises are negligible, one can obtain accurate, physically realizable, real-time estimates $\{\hat{x}(t), \hat{c}(t), \hat{z}(t)\}$ of the three state-vectors $\{x(t), c(t), z(t)\}$ as needed for implementation of optimal pointing/tracking controls (21) by using the command-state observer algorithm (23) and the composite-state observer algorithm (29), provided the state-equations for S are linearizable as in (26). If measurement noises associated with $y_{i,c}(t), y_i(t)$ are not negligible, the $(K_o, \bar{K}_o)$ matrices in (23), (29) should be determined by the formal procedures of Kalman Filtering Theory.

6.0 FORMULATION AND SOLUTION OF POINTING/TRACKING CONTROL PROBLEMS IN THE EXTENDED (x, c, z) STATE-SPACE

According to the command/disturbance uncertainty accommodation principle, and related arguments presented in Section 5.5, the design of high-performance, precision pointing/tracking control systems should be based on the real-time information embodied in the real-time values $x(t)$, $c(t)$, $z(t)$ of the three state-vectors x, c, z. That is, the designer should seek the pointing/tracking control law (algorithm) $u = u(?)$ in the form

$$u(t) = \mathcal{F}(x(t), c(t), z(t), t) \tag{33}$$

where observer-produced estimates $\hat{x}(t), \hat{c}(t), \hat{z}(t)$ are used to implement (33).

There are essentially two methodologies for designing extended-state pointing/tracking control laws of the type (33): (i) the optimal control method analogous to that used by Kalman for the problem (2)-(5), and (ii) a more fundamental and direct method involving linear algebra and basic linear stabilization techniques. In this section we will outline the essential features of both of those methodologies; further details may be found in [25], [26], [27].

6.1 _**An Extended-State Reformulation of Kalman's Optimal Pointing/Tracking Problem**_ - Kalman's absolute optimal, physically un-realizable, pointing/tracking problem (2)-(5) can be reformulated into a physically realizable, slightly less-than-optimal, problem by introducing the x, c, z state vectors, and the associated state models (2), (18), (20) with the sparse, unknown impulse-sequences $\sigma(t), \mu(t)$ ignored, [since there is no rational, scientific way (only "gambling" ways) to account for such uncertain $\sigma(t), \mu(t)$ in this, or any other, optimization procedure]. For this purpose, note

that the tracking error-vector e in (1),(3) can be rewritten in terms of (x, c, z) as follows

$$e = y_c - y$$

$$= Gc - Cx$$

$$= [-C \mid G \mid O] \begin{pmatrix} x \\ c \\ z \end{pmatrix}$$

Thus,

$$e = \bar{C}\tilde{x} ; \quad \bar{C} = \left[-C \mid G \mid O\right] ; \quad \tilde{x} = col.\left(x \mid c \mid z\right) \tag{34}$$

Moreover, the plant, command and disturbance models (2), (18), (20) can be combined into the one composite $\tilde{x}$ model

$$\left(\dot{\tilde{x}}\right) = \begin{bmatrix} A & O & FH \\ O & E & O \\ O & O & D \end{bmatrix} (\tilde{x}) + \begin{bmatrix} B \\ O \\ O \end{bmatrix} (u) + \begin{pmatrix} O \\ \mu(t) \\ \sigma(t) \end{pmatrix} \tag{35a}$$

$$y = [C \mid O \mid O] (\tilde{x}) \tag{35b}$$

and, using (34), the error/control quadratic performance criterion J in (3) can be rewritten in terms of $\tilde{x}$ as follows

$$J[u] = \tilde{x}^T(T)\,\bar{S}\tilde{x}(T) + \int_{t_o}^{T}\left[\tilde{x}^T\bar{Q}\tilde{x} + u^T Ru\right]dt ; \quad \begin{matrix} \bar{S} = \bar{C}^T S\bar{C} \\ \bar{Q} = \bar{C}^T Q\bar{C} \end{matrix} \tag{36}$$

The control $u(\cdot)$ that minimizes (36) for the composite plant/command/disturbance model (35) [with $\mu(t) \equiv 0$, $\sigma(t) \equiv 0$] can now be derived, <u>without</u> needing to know the future behavior of $y_c(t)$ and $w(t)$, using standard procedures of optimal control theory. This has been done in [25] with the result that the "less-than-absolute optimal," physically realizable, pointing/tracking control law (33), based on the extended (x,c,z) state-space, is given by

$$\hat{u}^o = -R^{-1}(t)B^T(t)\left[K_x(t)x + K_{xc}(t)c + K_{xz}(t)z\right] \tag{37}$$

where the three gain-matrices (K_x, K_{xc}, K_{xz}) are determined by reverse-time solution of the following, unilaterally-coupled matric differential equations [25; p. 349]

$$\dot{K}_x(t) = -K_x A - A^T K_x + K_x B R^{-1} B^T K_x - C^T Q C \quad ; \qquad K_x(T) = C^T S C \qquad (38a)$$

$$\dot{K}_{xc}(t) = -K_{xc} E - A^T K_{xc} + K_x B R^{-1} B^T K_{xc} + C^T Q G \quad ; \quad K_{xc}(T) = -C^T S G \qquad (38b)$$

$$\dot{K}_{xz}(t) = -K_x F H - A^T K_{xz} + K_x B R^{-1} B^T K_{xz} - K_{xz} D \quad ; \quad K_{xz}(T) = O \ . \qquad (38c)$$

Since the sub-absolute optimal problem (35),(36) is the same as Kalman's problem (2)-(5), with the exception that in solving (35),(36) the $\sigma(t)$, $\mu(t)$ impulses have been ignored, it is interesting to compare the structures of the two control algorithms. Comparing (6a,b) with (37),(38a) it is clear that one always obtains the equivalence

$$K_x(t) \equiv P(t) \quad \text{in (6a,b)} \ . \qquad (39)$$

Moreover, if in fact the sparse impulse-sequences $\sigma(t)$, $\mu(t)$ in (35) are actually zero, then it can be shown [28] that the following additional equivalence obtains

$$K_{xc}(t) c + K_{xz}(t) z \equiv -h(t) \quad \text{in (6a,c)} \qquad (40)$$

Finally, still assuming $\sigma(t) \equiv 0$, $\mu(t) \equiv 0$, it turns-out [25] that the extended state-space counterpart $\hat{J}^o$ of the "optimal performance" expression J^o in (7a), corresponding to (36), (37), (38), is given by

$$\hat{J}^o = x^T(t_o) K_x(t_o) x(t_o) + c^T(t_o) K_c(t_o) c(t_o) + 2 x^T(t_o) K_{xc}(t_o) c(t_o)$$
$$+ 2 \left[x^T(t_o) K_{xz}(t_o) + c^T(t_o) K_{cz}(t_o) \right] z(t_o) + z^T(t_o) K_z(t_o) z(t_o) \qquad (41)$$

where the additional matrices $K_{cz}(t)$, $K_c(t)$, $K_z(t)$ are determined by reverse-time solution of other matric differential equations similar to (38); see [25; Eq.(10)]. Note that, for fixed values of $x(t_o)$, $c(t_o)$, $z(t_o)$ and T, the "optimal" performance $\hat{J}_o$ in (41) will always be larger (less optimal) than J^o in (7a)

when the $\sigma(t)$, $\mu(t)$ impulses in (35) are <u>not</u> <u>identically zero</u>. In that case the difference $\mathcal{L}$ defined by

$$\mathcal{L} = \hat{J}^o - J^o \qquad (42)$$

is a direct measure of the pointing/tracking <u>performance loss</u> due to the inability of the physically realizable, sub-absolute optimal control $\hat{u}^o(t)$ in (37) to "see" the forthcoming, future impulse arrivals in $\sigma(t)$, $\mu(t)$. The practical implementation of (37) will, of course, require use of observer-generated real-time estimates $\hat{x}(t)$, $\hat{c}(t)$, $\hat{z}(t)$ as developed in Section 5.5.

An experimental comparison of Kalman's "absolute optimal" performance J^o in (7a) and the physically realizable sub-absolute "optimal" performance $\hat{J}^o$ achieved using the extended-state optimal control design method (35-(38), based on simulation studies of a particular example, is presented in [28]. For the several cases studied there, it turns-out that the physically <u>unrealizable</u> absolute optimal performance J^o is about 10-20% "better" (i.e. lower) than the physically realizable performance $\hat{J}^o$.

We will now describe an alternative and more fundamental method for designing pointing/tracking control systems in the extended $(x,c,z,)$ state-space. This alternative method does <u>not</u> involve optimal control ideas, and the introduction of a (potentially) "contrived" performance criterion J, but rather is based on simple linear-algebraic concepts and linear-stabilization techniques.

6.2 *An Algebraic-Stabilization Method for Pointing/Tracking Control Design in the Extended (x,c,z) State-Space* - The optimal control method outlined in Section 6.1 is an effective control design methodology because of the wide-spread popularity of Linear/Quadratic-type methods among today's

younger control designers and the wide-availability of a variety of (nearly automatic) CAD programs that are specifically tailored for executing Linear/Quadratic design procedures. On the other hand, such optimal control methods tend to relegate all conventional control design considerations (e.g. "setting-time," % overshoot, etc.) to the background and focus attention on mathematically minimizing the performance functional J. This introduces an extra layer of abstractions and mathematical complexities that can obscure the basic, underlying scientific features of the fundamental control problem being addressed. In this Section we will outline an alternative pointing/tracking control design method, for the extended (x,c,z) state-space, that is purely linear-algebraic and linear-stabilization in nature and that, like classical control methods, focuses on the essential, underlying features of pointing/tracking problems. Further details of this algebraic-stabilization method may be found in [26], [27], [28].

The algebraic-stabilization method of pointing/tracking control design for (2), (18), (20) [in (x,c,z)-space] begins by observing that the tracking error-vector $e(t) = y_c(t) - y(t)$ in (34) can become identically zero only if, for any arbitrarily given command-state $c = (c_1, \cdots, c_v)$, there exists a system-state vector x such that

$$Cx = Gc \ . \tag{43}$$

Satisfaction of the linear algebraic equation (43) is guaranteed if, and only if

$$rank[C \mid G] = rank[C] \tag{44}$$

which implies that G in (18) must allow the decomposition (factorization)

$$G = C\theta, \quad for \ some \ (perhaps \ non-unique) \ matrix \ \theta \ . \tag{45}$$

The fundamental requirement (44) is referred to as the "trackability condition," [26; Thm. 2]. We hereafter assume (44) is satisfied and, for

simplicity, that A, B, F, C, H, D are all constant; see [26] for the more general time-varying case. Next, we re-write e as follows

$$e = Gc - Cx$$
$$= C(\theta c - x)$$

$$e = Ce_{ss} \quad ; \quad e_{ss} = (\theta c - x) = \text{the "servo-state" vector}, \quad (46)$$

It is clear from (46) that the <u>basic requirement</u> for achieving precision pointing and tracking, $e(t) \approx zero$, is to control the auxiliary "servo-state" vector e_{ss} so that $e_{ss}(t)$ is promptly regulated <u>to</u>, and thereafter remains <u>in</u> (or very <u>near</u>), some subspace of the null-space $\mathcal{N}[C]$ of the given matrix C, while remaining acceptably bounded, in norm, at all times. Recall that $e_{ss} = 0$ is always a member of $\mathcal{N}[C]$; however, other values of $e_{ss} \neq 0$ may also lie in the linear space of vectors that comprises $\mathcal{N}[C]$, depending on the rank of C.

The state equation governing the motions of $e_{ss}(t)$ is readily computed to be

$$\dot{e}_{ss} = Ae_{ss} + (\theta E - A\theta)c - Bu - Fw(t) + \theta\mu(t) \qquad (47)$$

Thus, the control $u(\cdot)$ in (47) should be designed to promptly regulate $e_{ss} \rightarrow$ some subspace of $\mathcal{N}[C]$, between successive arrivals of the unknown impulses in $\sigma(t), \mu(t)$, while keeping $\|e_{ss}(t)\|$ acceptably bounded for all t. For this purpose, we will seek $u(\cdot)$ in the idealized, linear, extended-state feedback/feedforward form [26; eq. 36]

$$u = S_1 x + S_2 c + \Gamma z \qquad (48)$$

where the three constant gain-matrices S_1, S_2, Γ are to be designed as explained below.

Substitution of (48) into (47) yields the "closed-loop" equation of motion for $e_{ss}(t)$ as

$$\dot{e}_{ss} = (A + BS_1)e_{ss} + (\theta E - A\theta - BS_1\theta - BS_2)c - (B\Gamma + FH)z \qquad (49)$$

Thus, to achieve prompt regulation of $e_{ss}(t) \to S_{NC}$, $S_{NC} \subseteq$ some subspace of $\mathcal{N}[C]$, one should:

(i) Design S_1 so that all solutions $\tilde{e}_{ss}(t)$ of $\dot{\tilde{e}}_{ss} = (A + BS_1)\tilde{e}_{ss}$ are strongly asymptotically stable to some $S_{NC} \subseteq \mathcal{N}[C]$ and remain <u>norm-bounded</u>, at an acceptable level, for all t ; see [29] for the theory of "subspace stabilization." (50)

(ii) Design S_2 so that the vector $(\theta E - A\theta - BS_1\theta - BS_2)c$ always lies in $S_{NC} \subseteq \mathcal{N}[C]$, for <u>any</u> c. (51)

(iii) Design Γ so that the vector $(B\Gamma + FH)z$ always lies in $S_{NC} \subseteq \mathcal{N}[C]$, for <u>any</u> z . (52)

(iv) Re-check satisfaction of the boundedness condition in (i) and revise choice of S_{NC} and/or designs of S_1, S_2, Γ as needed; see [27]. (53)

These design requirements necessitate the trial-and-error choice of a suitable subspace $S_{NC} \subseteq \mathcal{N}[C]$ on which to "land" $e_{ss}(t)$, but otherwise involve only linear-algebraic considerations that can be achieved by straightforward, systematic procedures as explained in [26], [27], [29].

An overall block-diagram showing the control (48) implemented on the system (2) [using full-order command-state and composite system/disturbance state-observers (23), (29)] is shown in generic format in Figure 8. A specific 2nd-order example which illustrates this algebraic-stabilization design method is worked-out in detail in [26; p. 31].

7.0 SUMMARY AND CONCLUSIONS -

In this Chapter we have given a general description of a broad class of multi-input/multi-output pointing and tracking control problems encountered in industrial applications. The dynamic characteristics of the uncertain
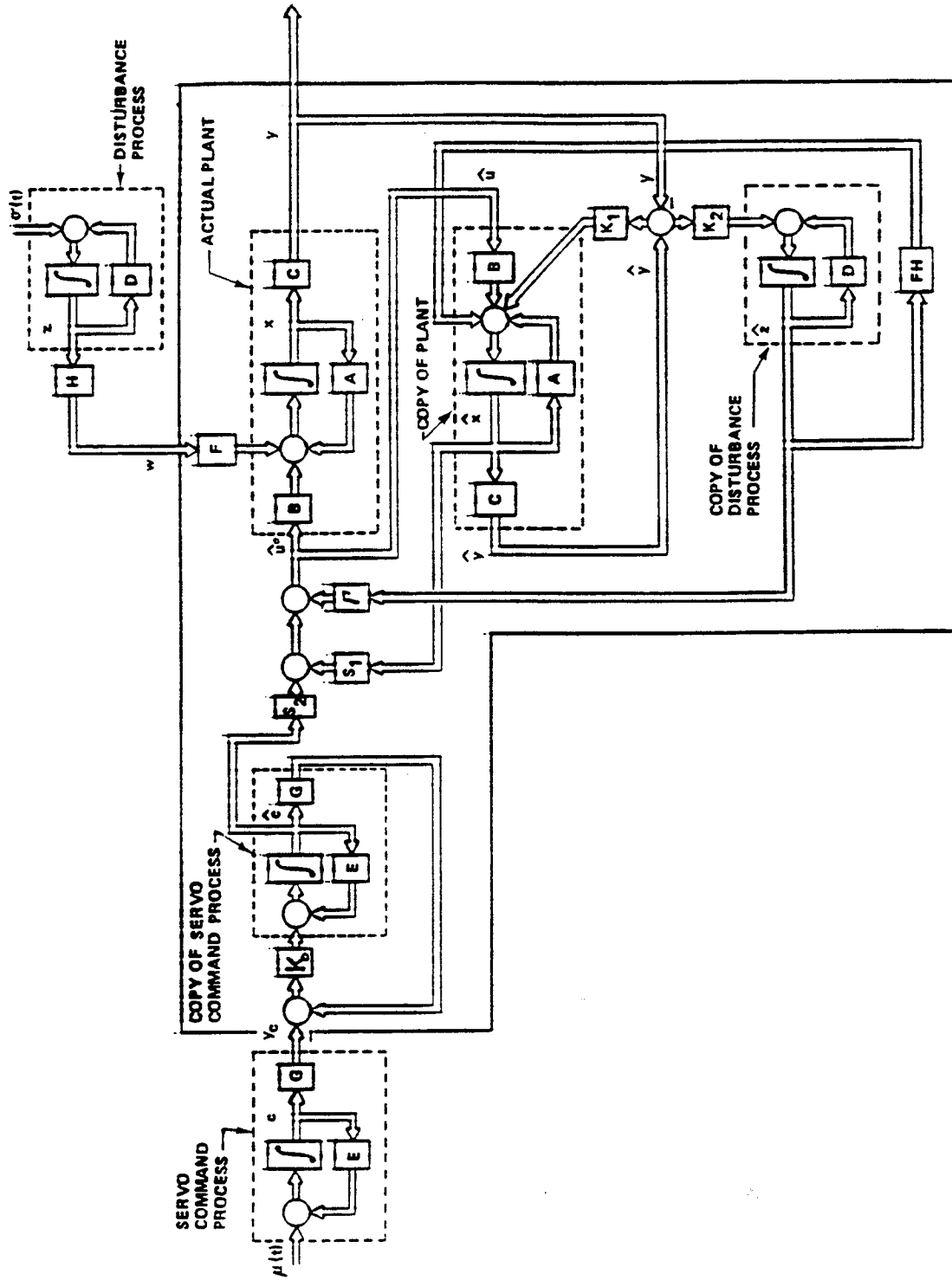
Figure 8 – Generic Block-Diagram of Dynamic system (2) with Tracking-Command Model (18), Disturbance Model (20), and (x, y, z)-Based Tracking control (48) with State Observers (23), (29).

commands and disturbances associated with those pointing/tracking problems have been analyzed from the information-theoretic viewpoint and some fundamental pointing/tracking performance limitations induced by those uncertainties have been identified. It has further been shown that the solution of a theoretical "absolute optimal" pointing/tracking control problem without such uncertainties, due to Kalman, can be used to quantify and evaluate numerically the extent of those uncertainty-related performance limitations, in any given application.

A relatively new form of mathematical model ("waveform-model"), which can simultaneously represent trend behavior and uncertainty in realistic pointing/tracking commands and disturbances, has been used to obtain a command state-vector $c(t)$ and disturbance state-vector $z(t)$, and associated state-variable models, that can effectively represent the characteristic dynamic time-behavior of uncertain commands and disturbances in pointing/tracking problems. A fundamental principle, called the "command/disturbance uncertainty accommodation principle," has been used to assert that an optimal, physically realizable, rational control law (algorithm) for a pointing/tracking control problem must be based on the real-time values of the current system-state $x(t)$, the current command-state $c(t)$ and the current disturbance-state $z(t)$. Two different control design methodologies, a variation of Kalman's optimal control method and a purely linear-algebraic method, for deriving such pointing/tracking controllers have been outlined.

The fundamental principles and performance limitation ideas presented here, together with the extended-state (x,c,z) problem formulations and associated control design methodologies in Section 6.0, should enable the

attainment of maximum, physically realizable performance levels in a broad class of precision pointing/tracking control problems with uncertain commands and disturbances.

The ideas presented here can be readily adapted to the design of digital (discrete-time) pointing/tracking control systems by following the procedures given in [14]. It is remarked that the use of a digital control system in pointing and tracking problems introduces an additional degree of performance limitation owing to the imposition of a specified sequence of discrete times t_j at which the (otherwise "open-loop") discrete control actions are allowed to be updated. An effective technique for mitigating that additional performance limitation is described in [14; p. 311], [30].

REFERENCES

1. E. Wong and B. Hajek, *Stochastic Processes in Engineering Systems*, Springer-Verlag, NY, 1985.

2. R. Stengel, *Stochastic Optimal Control; Theory and Application*, Wiley-Interscience, NY, 1986.

3. R. E. Kalman, "The Theory of Optimal Control and the Calculus of Variations," *Proc. of the Symposium on Mathematical Optimization Techniques*,RAND Corp. Rpt. No. R-396-Pr, 1963, Santa Monica, CA; also published in book format by University of CA, Berkeley Press, 1963.

4. C. D. Johnson, "Accommodation of Disturbances in Optimal Control Problems.", *International Journal of Control*, Vol. 15, No. 2, pp. 209-231, 1972; also, *Proc. Third Southeastern Symposium on System Theory*, Atlanta, GA, April 1971.

5. J. Haberstock and C. D. Johnson, "Disturbance-Utilizing Control for Linear Systems with Non-Quadratic Performance Indices," *Proc. 1988 Southeastern Symposium on System Theory (SSST)*, Charlotte, NC, p. 280, March 1988.

6. A. E. Bryson, Jr. and Y. C. Ho, *Applied Optimal Control*, Blaisdell Publishing Co., Waltham, MA, 1969.

7. D. Pierre, *Optimization Theory with Applications*, John Wiley, NY, 1969; also published in paperback by Dover, 1986.

8. R. Bellman, *Dynamic Programming*, Princeton University Press, Princeton, NJ, 1957.

9. J. T. Oden, *Finite Elements of Nonlinear Continua*, McGraw-Hill Book Co., NY, 1971.

10. C. D. Johnson, "Optimal Control of the Linear Regulator with Constant Disturbances," *IEEE Trans. on Automatic Control*, Vol. AC-13, No. 4, pp. 416-412, August 1988.

11. C. D. Johnson, "Further Study of the Linear Regulator with Disturbances: The Case of Vector Disturbances Satisfying a Linear Differential Equation," *IEEE Trans. on Automatic Control*, Vol. AC-15, No. 2, pp. 222-228, April 1970.

12. C. D. Johnson, "Accommodation of Disturbances in Linear Regulator and Servo-Mechanism Problems," *IEEE Trans. on Automatic Control*, (Special Issue on the "Linear- Quadratic-Gaussian Problem"), Vol. AC-16, No. 6, p. 635, December 1971.

13. C. D. Johnson, Theory of Disturbance Accommodating Controllers, Chapter 7 in the book: *Advances in Control and Dynamic Systems*, Vol. 12, Edited by C. T. Leondes, Academic Press, 1976.

14. C. D. Johnson, "Discrete-Time Disturbance-Accommodating Control Theory," Chapter in the book *Control and Dynamic Systems: Advances in Theory and Applications*, Academic Press, NY, Vol. 18, 1982.

15. C. D. Johnson, "Disturbance-Accommodating Control; An Overview," *Proc. of the 1986 American Control Conference*, Seattle, WA, p. 526, 1986.

16. W. Brogan, *Modern Control Theory*, Quantum Pub., Inc., NY, 1974.

17. C. D. Johnson, "State Overdescription and Uncontrollability of Dynamical Systems; Part I, Non-Linear Systems," *Int'l Journal of Control*, Vol. 19, No. 2, pp. 225-242, February 1974.

18. C. D. Johnson, "State Overdescription and Uncontrollability of Dynamical Systems; Part II, Linear Systems," *Int'l Journal of Control*, Vol. 19, No. 6, pp. 1087-1100, June 1974.

19. C. D. Johnson, "Overmodeling of Dynamical Processes," *Proc. of the Fifth Pittsburgh Conf. on Modeling and Simulation*, Pittsburgh, PA, April 24-26, 1974.

20. C. D. Johnson, "Modes of Overmodeling," *Proc. of the Sixth Pittsburgh Conference on Modeling and Simulation*, Pittsburgh, PA, April 24-25, 1975.

21. R. Brown and P. Hwang, *Introduction to Random Signals and Applied Kalman Filtering* (2nd Ed.), John Wiley, NY, 1992.

22. C. D. Johnson, "On Observers for Systems with Unknown Inaccessible Inputs," *Int'l. Journal of Control*, Vol. 21, No. 5, pp. 825-831, 1975.

23. C. D. Johnson, "Disturbance-Utilizing Control for Noisy Measurements and Disturbances; Part I: The Continuous-Time Case," *Int'l. Journal of Control*, Vol. 39, No. 5, pp. 859-868, 1984.

C-2

24. C. D. Johnson, "Disturbance-Utilizing Control for Noisy Measurements and Disturbances; Part II: The Discrete-Time Case," *Int'l. Journal of Control*, Vol. 39, No. 5, pp. 869-877, 1984.

25. C. D. Johnson, "Utility of Disturbances in Disturbance-Accommodating Control Problems," *Proc. of the 15th Annual Meeting of the Society for Engineering Science*, Gainesville, FL, p. 347, December 1978.

26. C. D. Johnson, "Algebraic Solution of the Servomechanism Problem with External Disturbances," *A.S.M.E. Trans, Journal of Dynamic Systems, Measurements, and Control*, Series G, Vol. 96, No. 1, pp. 25-35, March 1974.

27. C. D. Johnson, "An Improved Computational Procedure for 'Algebraic Solution of the Servo-Mechanism Problem with External Disturbances," *A.S.M.E. Trans, Journal of Dynamic Systems, Measurements, and Control*, Series G, Vol. 97, No. 2, pp. 161, 1975.

28. R. Dharia and C. D. Johnson, "On the Theoretical Sub-Optimality of Optimal Disturbance-Utilizing Control Laws," *Proc. 1992 IEEE Southeastcon Conf.*, Birmingham, AL, Vol. 2, p. 812, April 1992.

29. C. D. Johnson, "Stabilization of Linear Dynamical Systems with Respect to Arbitrary Linear Subspaces," *Journal of Mathematical Analysis and Application*, Vol. 44, No. 1, p. 175, October 1973.

30. C. D. Johnson and N. Kheir, "An Optimal Holding Strategy for Discrete-Time MIMO Servo-Tracking Controllers," in *Fundamentals of Discrete-Time Systems* (book), TSI Press, Albuquerque, NM, 1993.